Combining nuclear theory and neutron star observations to determine the properties of dense matter

Andrew W. Steiner (UTK/ORNL)

July 11, 2016

With: Edward F. Brown, Farrukh J. Fattoyev, Tobias Fischer, Stefano Gandolfi, Sophia Han, Matthias Hempel, Jari J.E. Kajava, James M. Lattimer, Joonas Nättilä, William G. Newton, Juri Poutanen, Valery F. Suleimanov

Outline

- Dense matter
- Speed of sound
- Masses and radii
- Bayesian inference
- QLMXBs and PRE X-ray bursts
- Universal relations and correlations

Neutron Star Composition

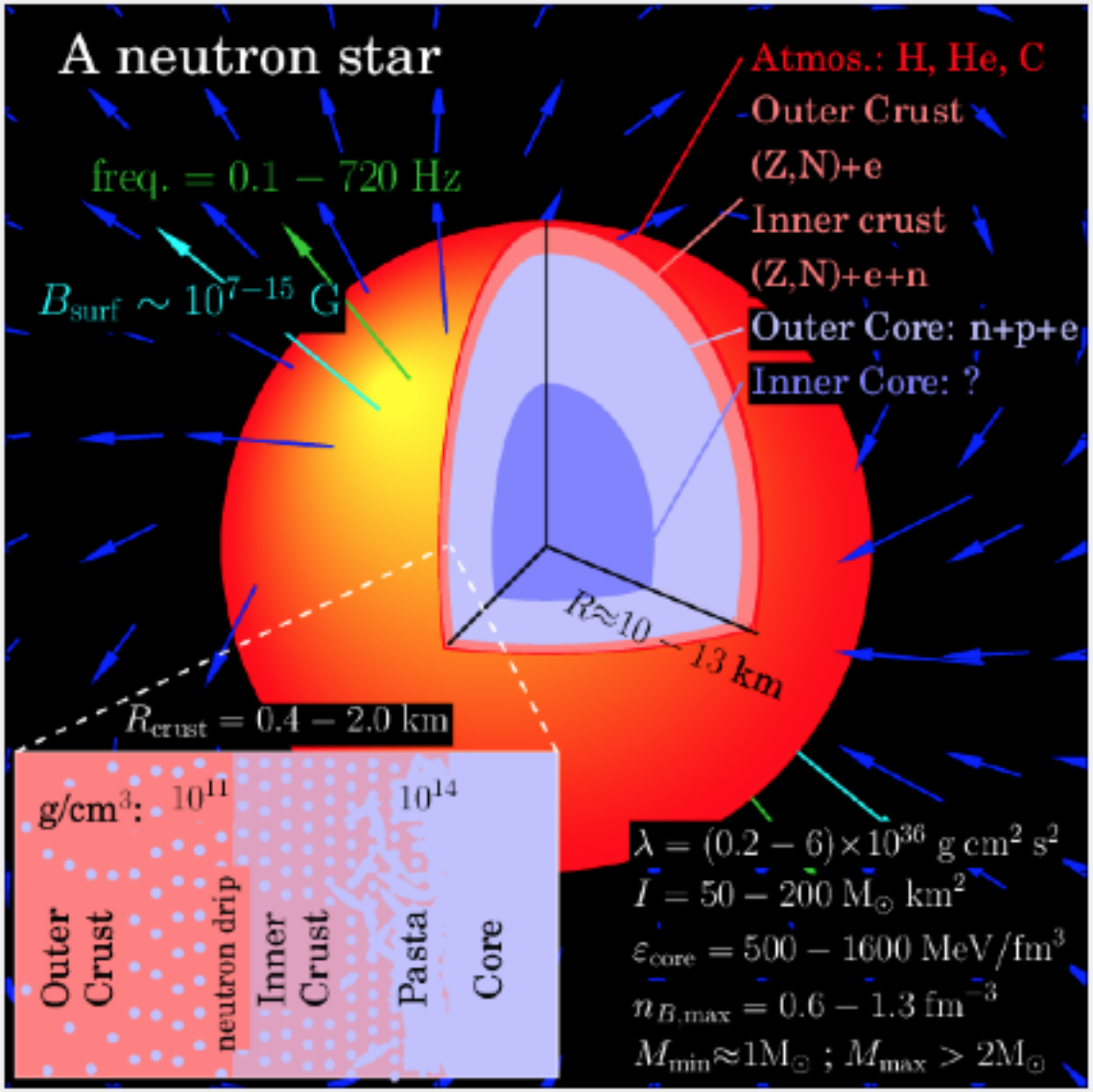

Inspired by D. Page; open source (python)

- Outer crust: of neutron-rich nuclei $\mu_n = \mu_p + \mu_e$
- Inner crust: neutron-rich nuclei embedded in a sea of quasi-free superfluid neutrons
- Outer core: fluid of neutrons, protons, and electrons
- Inner core: hyperons? Bose condensates? deconfined quark matter?

What are the correct degrees of freedom for the effective field theory which describes dense matter?

Neutron Star Masses and Radii and the EOS

- Neutron stars (to better than 10%) all lie on one universal mass-radius curve
  (Largest correction is rotation)

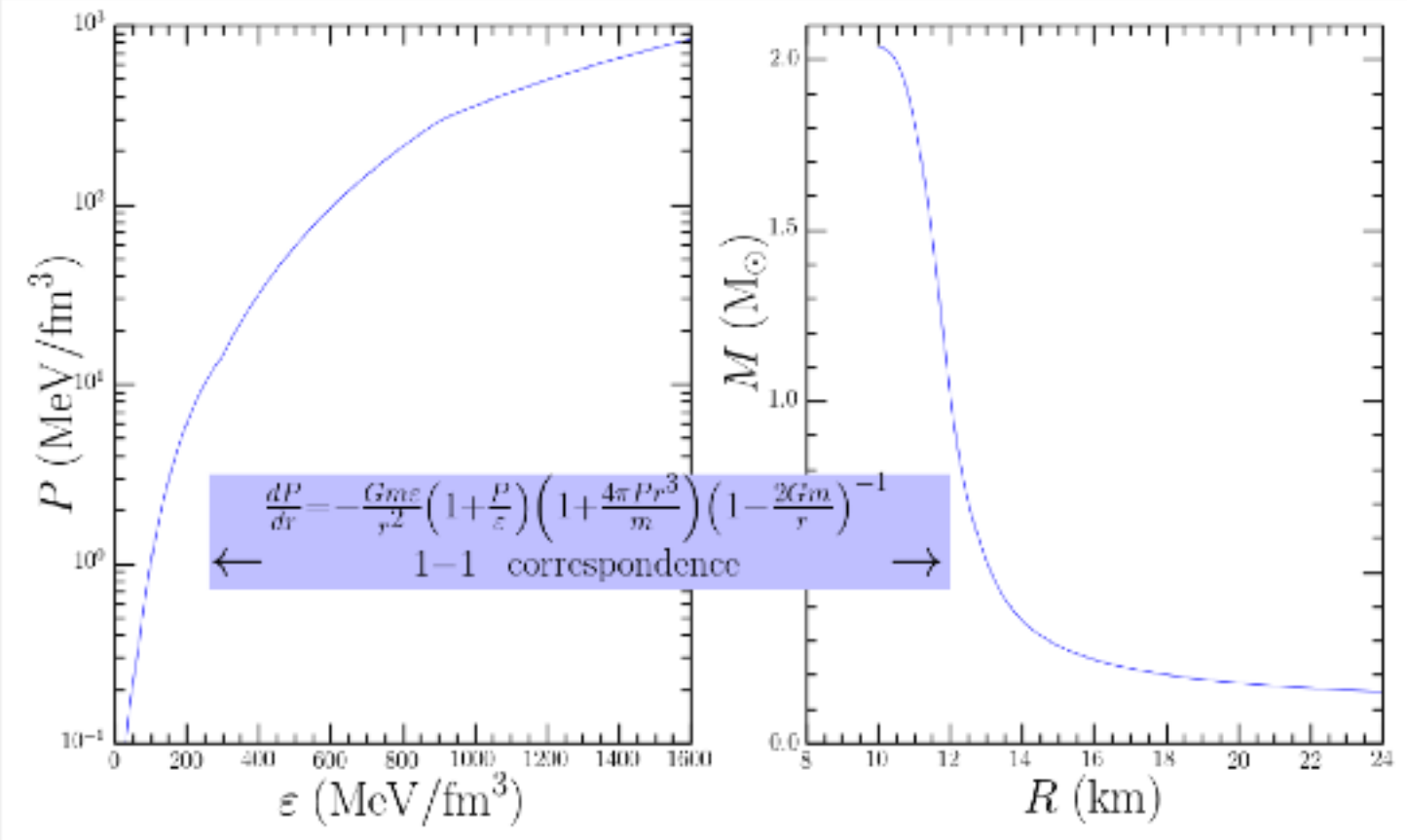

- Two 2 $M_\odot$ neutron stars
  Demorest et al. (2010), Antoniadis et al. (2013)
- As of 2007, neutron star radii ranged from 8-16 km
  Lattimer and Prakash (2007)
- Now 10-13 km is more likely
  Steiner, Lattimer, and Brown (2013)

Speed of sound

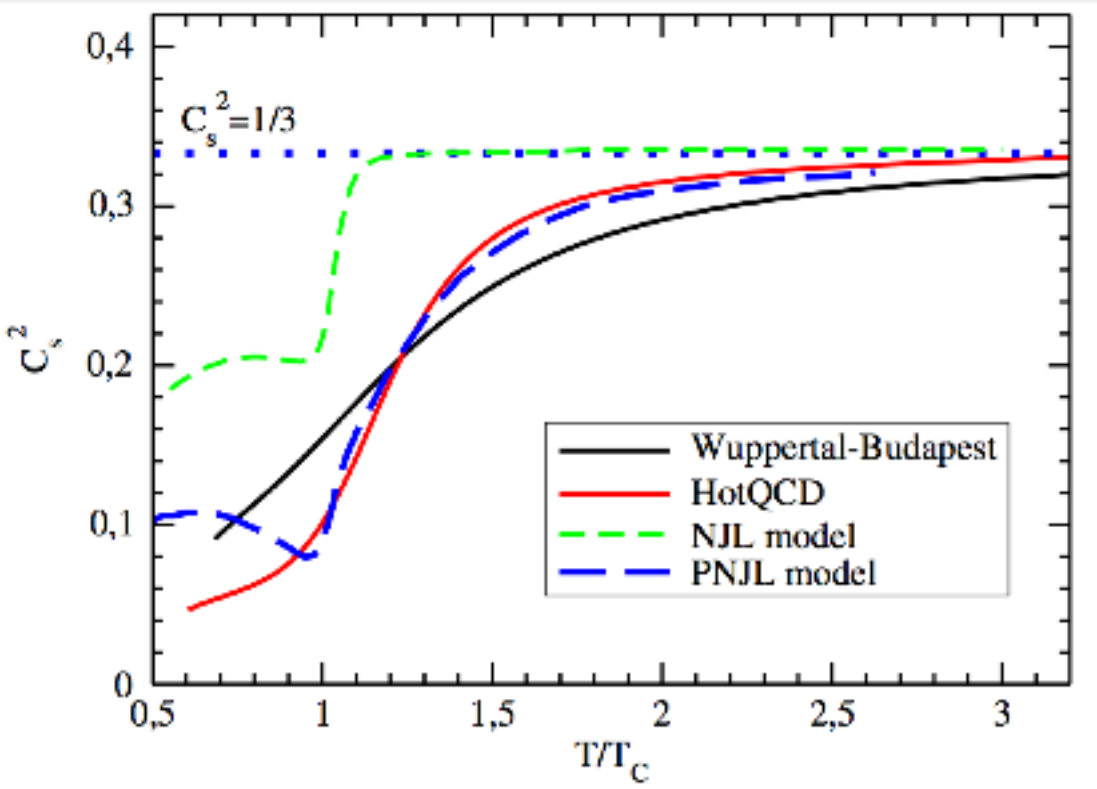

FIG. 4 (color online). Speed of sound squared as a function of T/T_C. The red solid curve corresponds to the HotQCD data, the black solid one to the Wuppertal-Budapest data, the short-dashed one to the NJL model, and the long-dashed one to the Polyakov loop extended NJL model fit to the HotQCD lattice data.

Plumari et al. (2011)

- The speed of sound at zero density and finite temperature: $c_s^2 \to 1/3$ as $T \to \infty$
- What happens at high density and zero temperature?
- Perturbation theory suggests c_s^2 increases to 1/3 from below
  Kurkela et al. (2010)
- $c_s^2 \approx 1/12$ in neutron matter at the saturation density
- Is $c_s^2 > 1/3$ anywhere in the universe?

Assume $c_s^2 < 1/3$ everywhere

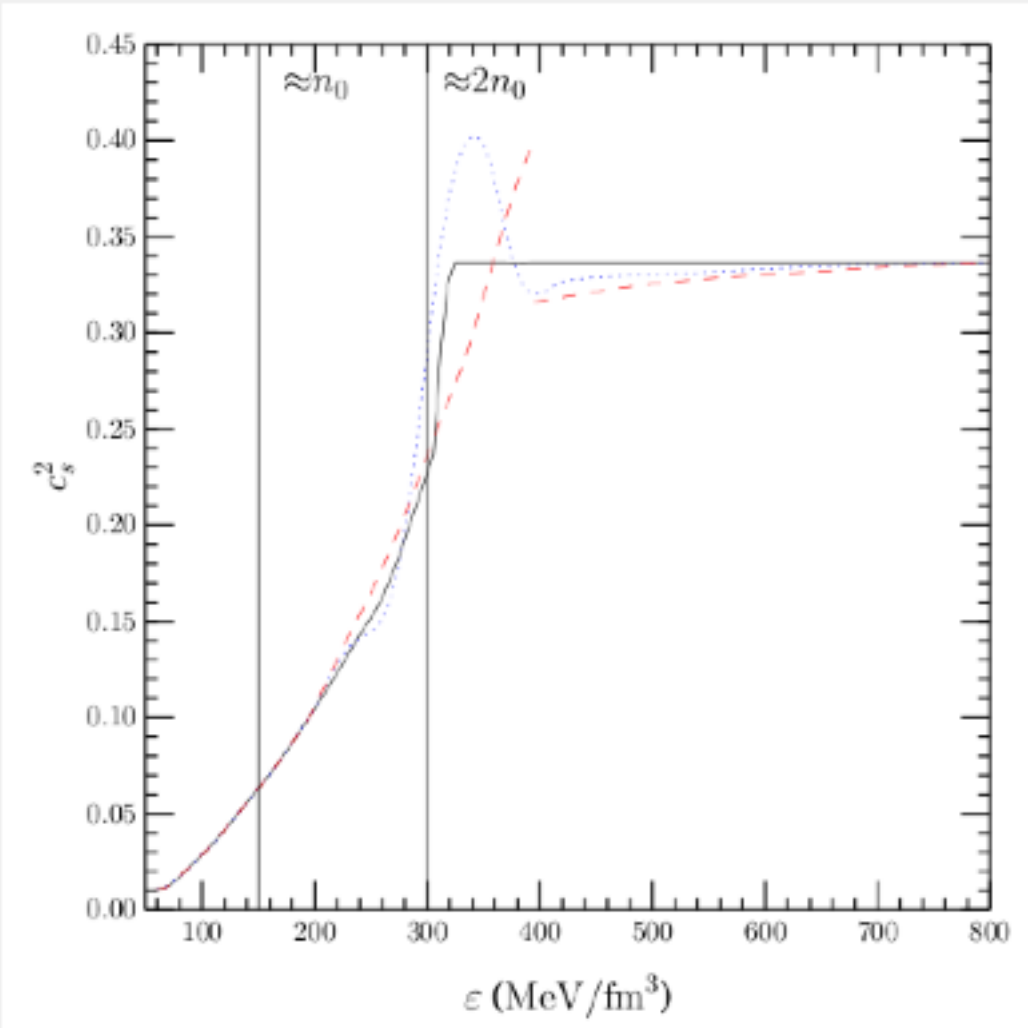

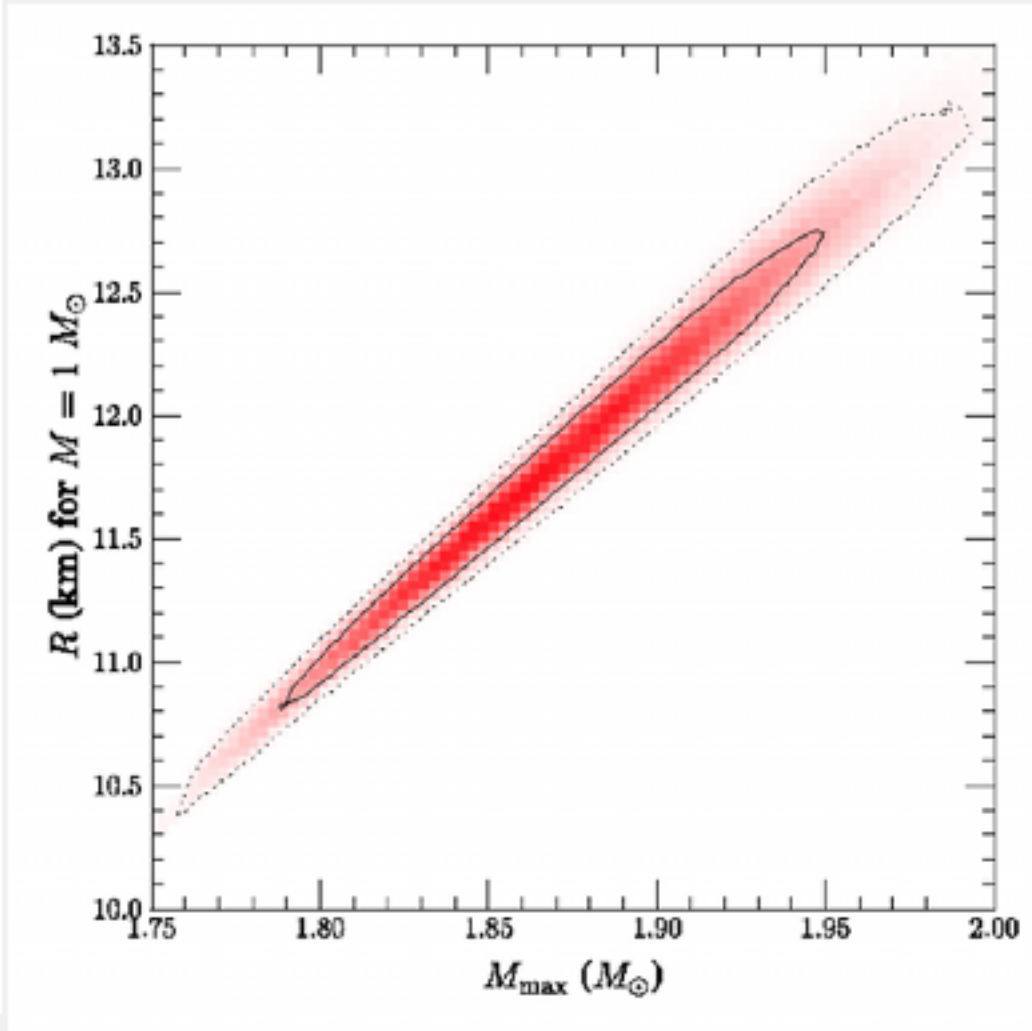

Bedaque and Steiner (2015)

- Assume the speed of sound as large is maximal, but $< 1/3$ (black curve)
- No! Not unless R is large. c_s^2 must be non-trivial at high densities. Why?
- Implies a phase transition at high-density, or a some new length scale

Neutron Star Masses and Radii and the EOS

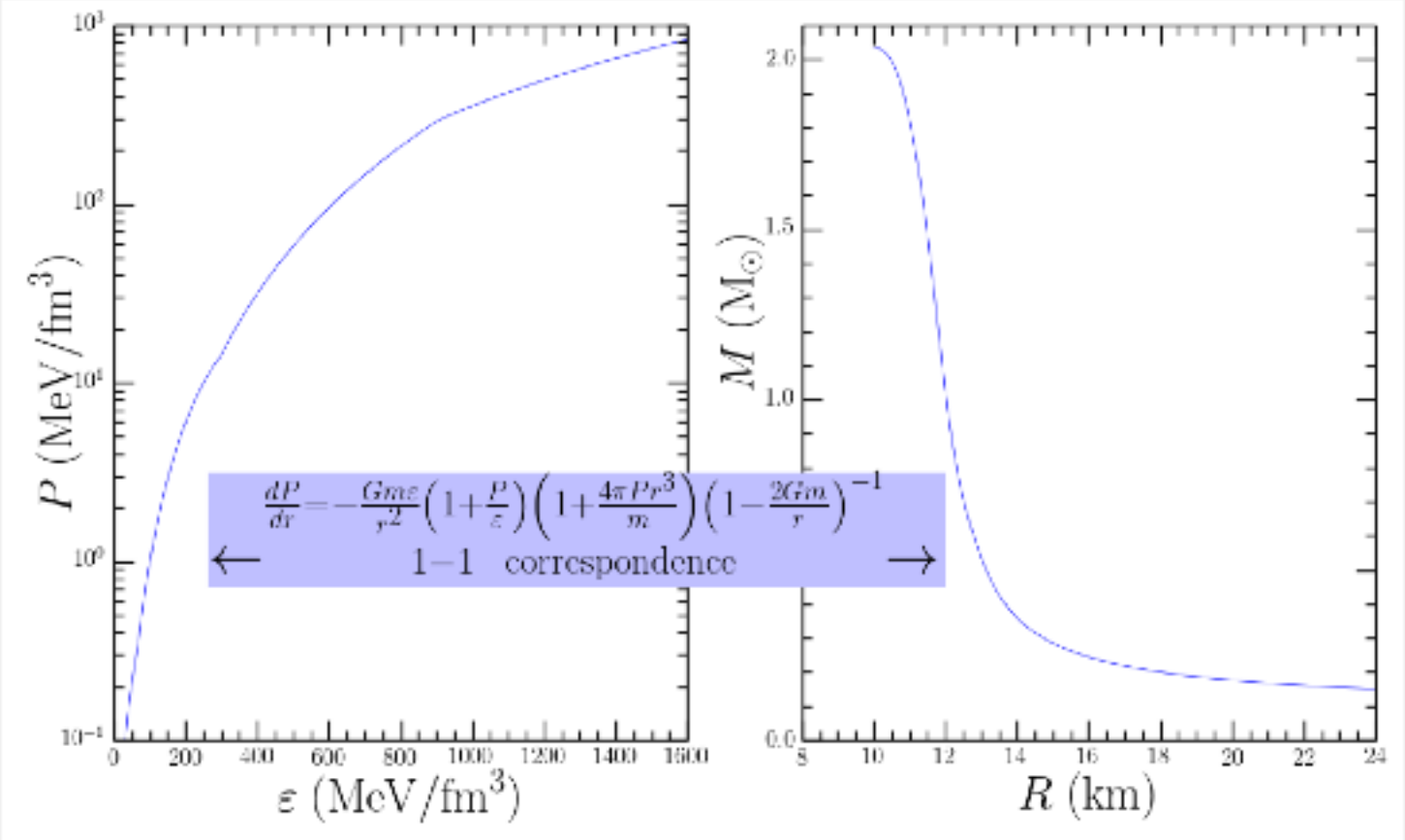

- How do we actually obtain constraints on the EOS from observations?
- Problem #1: Data is not that precise (as opposed to accurate)

Bayesian Inference for Masses and Radii

- Problem #2: It is a fully two-dimensional fitting problem

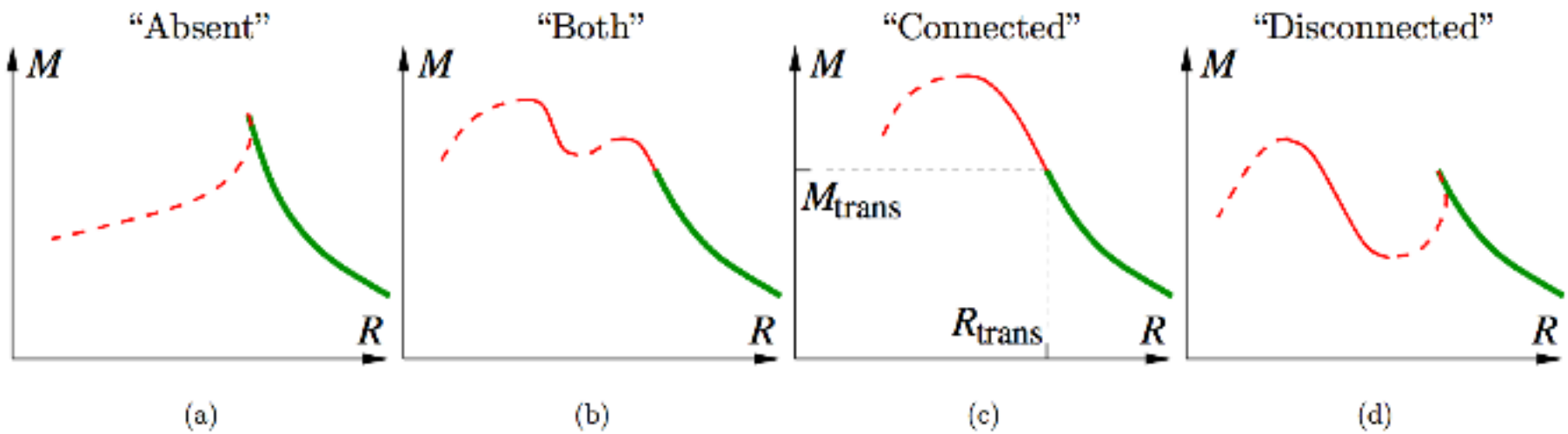

FIG. 2: Four possible topologies of the mass-radius relation for hybrid stars. The thick (green) line is the hadronic branch. Thin solid (red) lines are stable hybrid stars; thin dashed (red) lines are unstable hybrid stars. In (a) the hybrid branch is absent. In (c) there is a connected branch. In (d) there is a disconnected branch. In (b) there are both types of branch. In realistic neutron star $M(R)$ curves, the cusp that occurs in cases (a) and (d) is much smaller and harder to see [13, 14]

Alford et al. (2013)

- Mass-radius relation may be double-valued in either mass or radius
- Is a curve more likely if it passes through the observed data point multiple times?
- Solution! Bayesian inference: "Bayesian Methods in Nuclear Physics" at the INT

  There are frequentist solutions as well.

Bayesian Inference vs. χ^2 fitting

$$\chi^2 = \sum_i \left[\frac{(\text{data})_i - (\text{model})_i}{(\text{err})_i} \right]^2$$

- Maximize the likelihood: $\mathcal{L} = \exp(-\chi^2/2)$ with respect to model parameters
- Not unique when uncertainties in independent variable are large
- Bayes theorem: $P[\mathcal{M}_i|D] \propto P[D|\mathcal{M}_i]P[\mathcal{M}_i] = \mathcal{L} \times \text{prior}$
- Determine parameters through marginalization, i.e.

$$P(\mathcal{M}_i^0) = \int \delta(\mathcal{M}_i - \mathcal{M}_i^0) P[D|\mathcal{M}_i] P[\mathcal{M}_i] \, d\mathcal{M}$$

- Integrals can be computationally demanding
- Reproduces traditional χ^2 fit in the appropriate limits

Gaussian Approximation

- $\mathcal{L} = \exp(-\chi^2/2)$, so if if χ^2 is nearly quadratic near the minimum then the likelihood is Gaussian in the model parameters
  Common assumption in frequentist approaches
- If this approximately holds, the covariance matrix is related to the second derivatives
- This approximation can fail badly
- Important for MC simulation of uncertainties; covariance matrix doesn't contain all the information

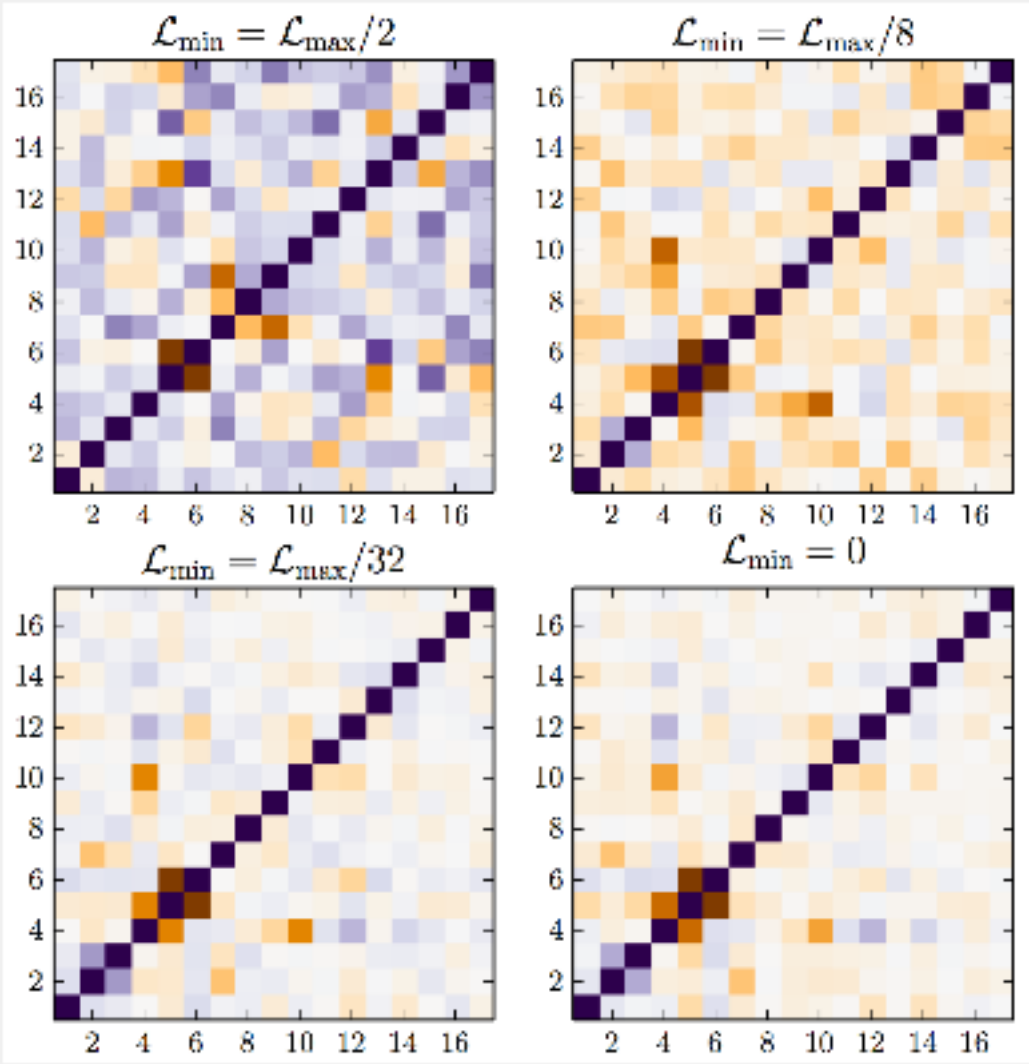

Covariance matrices from a fit to neutron star mass and radius data. Upper-left is near best-fit, lower-right is full likelihood.
Steiner (2015)

Model Comparison and Bayes Factors

- Frequentist: smallest χ^2 wins (likelihood ratio test)
- Only the value of $\mathcal{L}$ at the best fit parameter set is relevant
- Bayesian: compute evidence

$$E[\mathcal{M}] = \int P[D|\mathcal{M}_i]P[\mathcal{M}_i]\, d\mathcal{M}$$

- Bayes factor = ratio of two evidence integrals
- B > 10 indicates a strong preference for the model in the numerator
  Bayes factors work just like gambling odds
- Bayes factors can automatically disfavor models with too many parameters
  In detail, we employ Bayesian model averaging

My picture of what NS radii look like

Posterior Confidence Ranges and Evidence Integrals

Model	N_H	Dist.	Comp.	$R_{1.4}$ (km)	I
Base	G13	G13	H	11.11–11.88	$(1.77 \pm 0.09) \times 10^{-8}$
Base	G13	G13	H+He	11.36–12.84	$(4.50 \pm 0.21) \times 10^{-3}$
Base	G13	Alt	H	10.73–11.65	$(1.86 \pm 0.18) \times 10^{-6}$
Base	G13	Alt	H+He	11.45–13.32	$(3.71 \pm 0.21) \times 10^{-1}$
Base	G13	H10	H	10.77–11.71	$(1.23 \pm 0.09) \times 10^{-7}$
Base	G13	H10	H+He	11.36–13.44	$(4.28 \pm 0.35) \times 10^{-3}$
Base	D90	G13	H	10.67–11.51	$(4.65 \pm 0.48) \times 10^{-3}$
Base	D90	G13	H+He	11.31–12.64	$(2.14 \pm 0.19) \times 10^{+2}$
Base	D90	Alt	H	10.85–11.79	$(9.40 \pm 1.22) \times 10^{-3}$
Base	D90	Alt	H+He	11.37–12.61	$(4.06 \pm 0.36) \times 10^{+2}$
Base	D90	H10	H	10.78–11.70	$(4.78 \pm 0.73) \times 10^{-3}$
Base	D90	H10	H+He	11.23–12.62	$(1.57 \pm 0.07) \times 10^{+2}$
Base	H10	G13	H	10.87–11.82	$(1.04 \pm 0.08) \times 10^{+0}$
Base	H10	G13	H+He	11.15–12.38	$(1.84 \pm 0.12) \times 10^{+2}$
Base	H10	Alt	H	11.03–12.07	$(1.39 \pm 0.20) \times 10^{+2}$
Base	H10	Alt	H+He	11.04–12.31	$(1.44 \pm 0.10) \times 10^{+2}$
Base	H10	H10	H	10.78–11.95	$(7.52 \pm 0.65) \times 10^{+1}$
Base	H10	H10	H+He	11.31–12.66	$(5.30 \pm 0.22) \times 10^{+2}$
Exo	G13	G13	H	9.15–10.81	$(7.32 \pm 0.63) \times 10^{-6}$
Exo	G13	G13	H+He	10.52–11.77	$(4.46 \pm 0.38) \times 10^{-2}$
Exo	G13	Alt	H	10.42–11.39	$(1.21 \pm 0.19) \times 10^{-3}$
Exo	G13	Alt	H+He	10.88–12.59	$(7.33 \pm 0.78) \times 10^{-1}$
Exo	G13	H10	H	10.61–11.41	$(2.23 \pm 0.48) \times 10^{-5}$
Exo	G13	H10	H+He	10.76–12.38	$(1.67 \pm 0.16) \times 10^{-2}$
Exo	D90	G13	H	9.39–10.97	$(5.46 \pm 1.74) \times 10^{-1}$
Exo	D90	G13	H+He	10.53–12.45	$(2.29 \pm 0.13) \times 10^{+1}$
Exo	D90	Alt	H	9.86–11.44	$(3.04 \pm 0.42) \times 10^{-1}$
Exo	D90	Alt	H+He	10.90–12.31	$(4.46 \pm 0.22) \times 10^{+1}$
Exo	D90	H10	H	9.60–11.38	$(2.27 \pm 0.50) \times 10^{-1}$
Exo	D90	H10	H+He	10.61–12.28	$(2.59 \pm 0.15) \times 10^{+1}$
Exo	H10	G13	H	9.87–11.49	$(5.15 \pm 0.51) \times 10^{+0}$
Exo	H10	G13	H+He	10.60–11.99	$(4.67 \pm 0.46) \times 10^{+1}$
Exo	H10	Alt	H	10.45–11.74	$(5.17 \pm 0.64) \times 10^{+1}$
Exo	H10	Alt	H+He	10.53–11.81	$(7.49 \pm 0.75) \times 10^{+1}$
Exo	H10	H10	H	10.42–11.72	$(2.83 \pm 0.21) \times 10^{+1}$
Exo	H10	H10	H+He	10.74–12.39	$(8.93 \pm 0.47) \times 10^{+1}$

Lattimer and Steiner (2014)

- We try several models, each with $\sim 10^{5-6}$ solutions of the TOV equations
- Model-to-model variation provides estimates of systematics
- Compute evidence for each model
  Compute Bayes factors from these results
- Not all systematic uncertainties are easily handled this way

Low-mass X-ray binaries

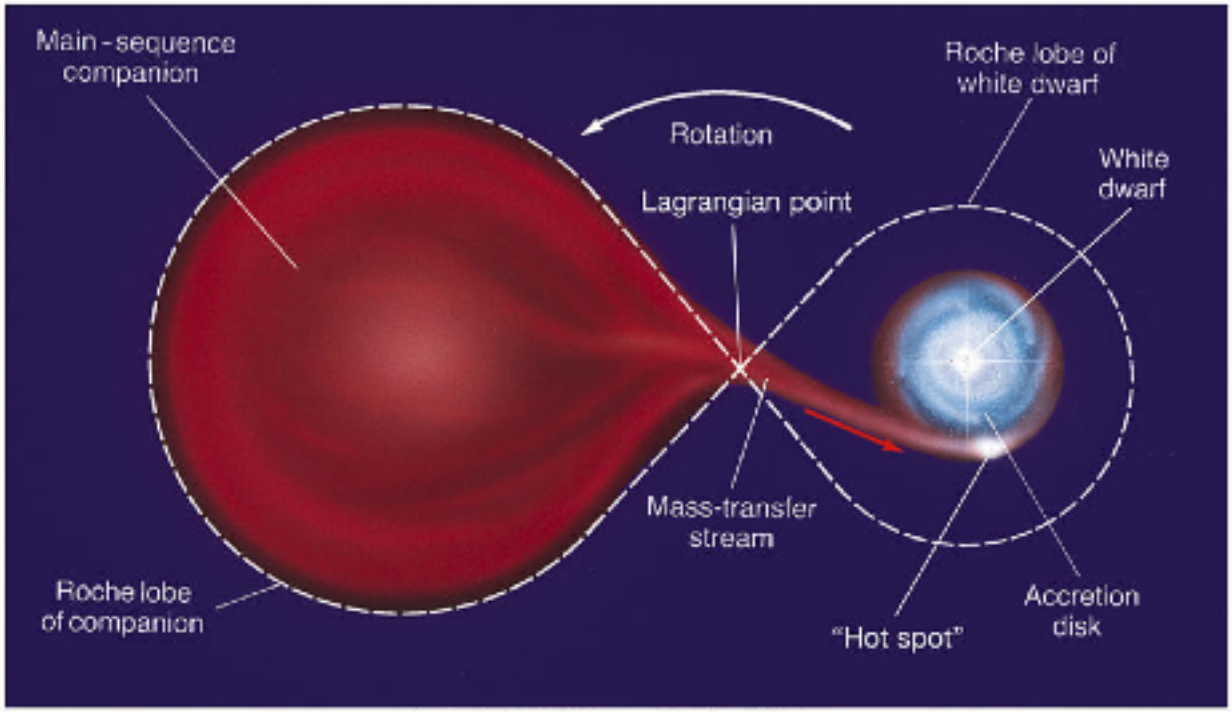

Copyright © 2005 Pearson Prentice Hall, Inc.

- H and He accreted is unstable
- Accretion is unstable and sporadic
- X-ray burst, burns H and He to heavier elements

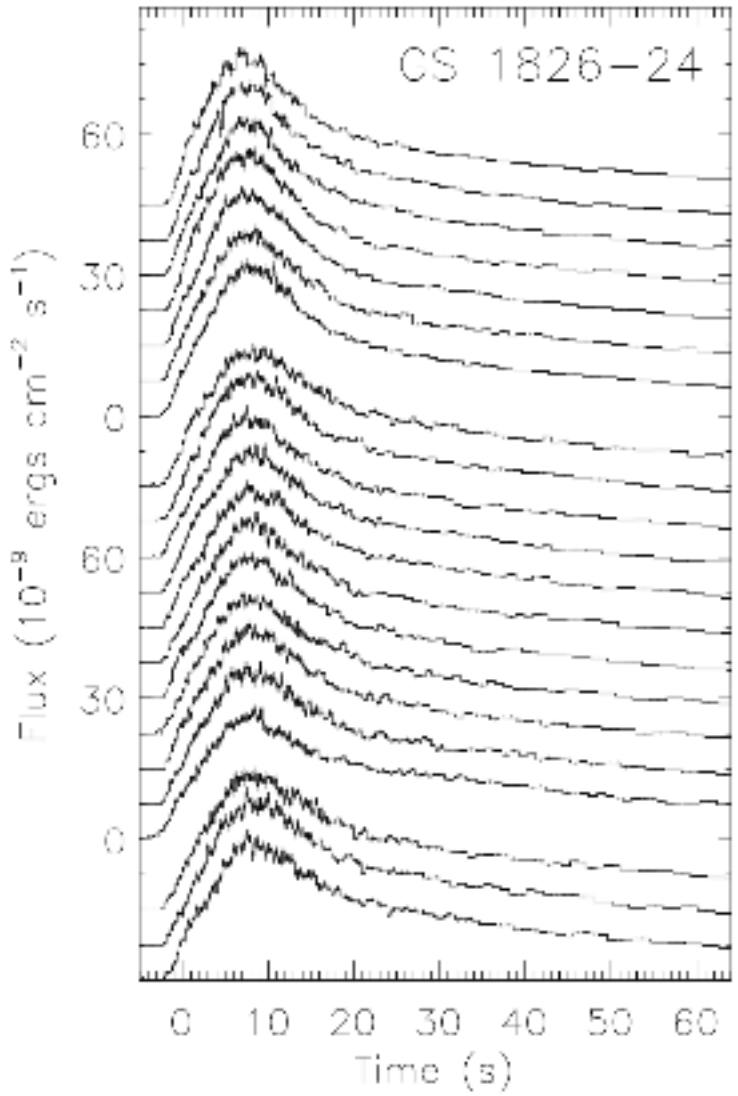

FIG. 1.— Profiles of 20 X-ray bursts from GS 1826−24 observed by *RXTE* between 1997–2002, plotted with varying vertical offsets for clarity. The upper group of 7 bursts were observed in 1997–98, the middle group of 10 bursts in 2000, while the lower group of 3 were observed in 2002. The bursts from each epoch have been time-aligned by cross-correlating the first 8 seconds of the burst. Error bars indicate the 1σ uncertainties.

X-ray bursts from GS 1826-24 from Galloway et al. (2004)

Radius Measurements in qLMXBs

Quiescent LMXBs

- Blackbody-like spectrum of X-rays

$$F \propto T_{\text{eff}}^4 \left(\frac{R_\infty}{D} \right)^2$$

e.g. Rutledge et al. (1999)

Several systematics:

- Distance
- X-ray absorption
- Atmosphere composition
- Area of emitting surface
- No model-independent way of fitting the data

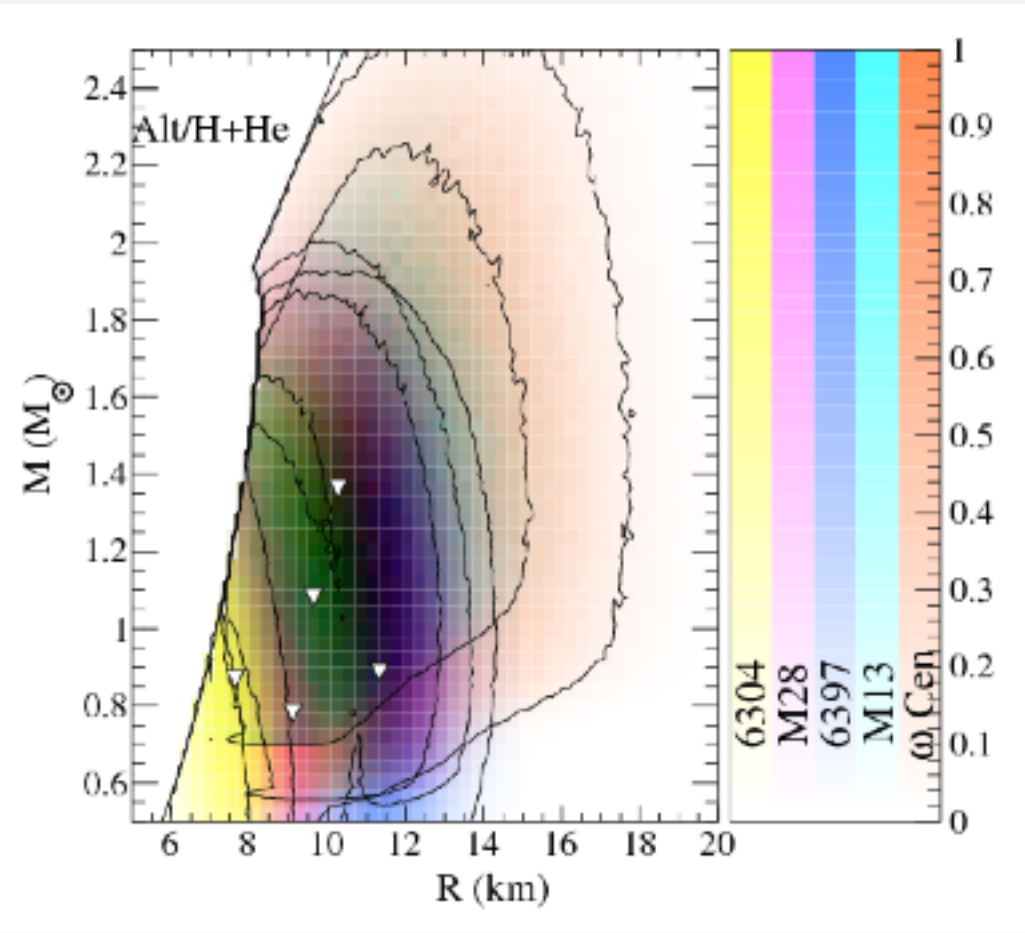

Lattimer and Steiner (2014) - Probability distributions for five neutron stars, colors added together

Photospheric Radius Expansion X-ray Bursts

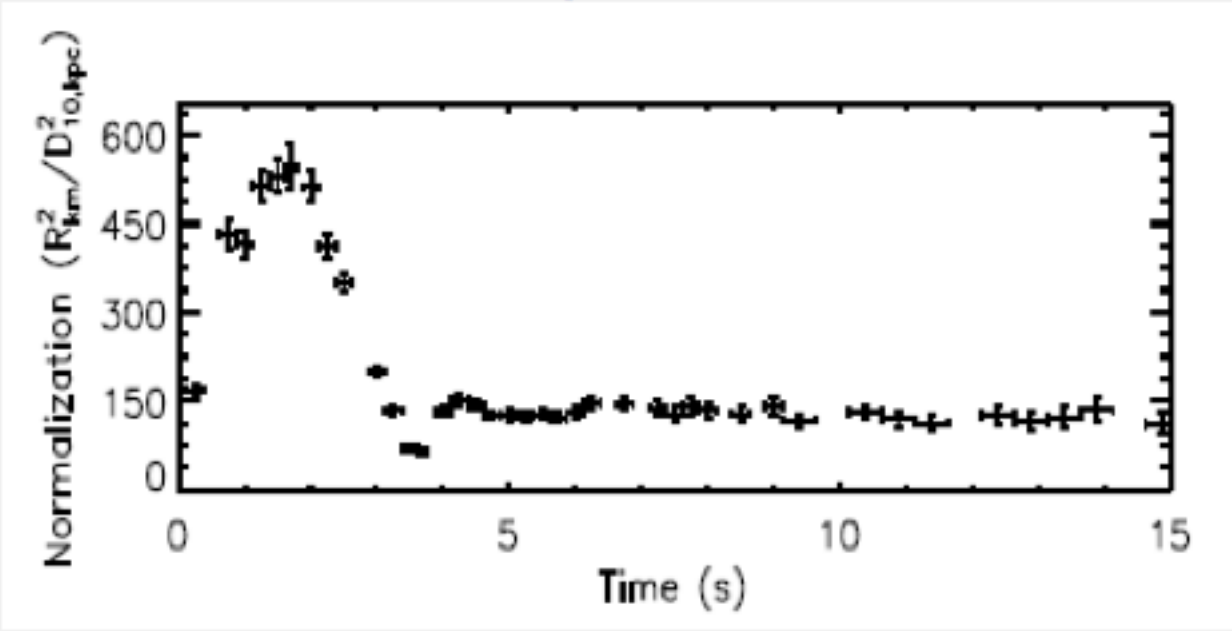

EXO 1745-248 from Özel, Güver, and Psaltis (2009)

- Central idea: balance between radiation pressure and gravity provides a new calibration point
- Use "hard-state" bursts to ensure accretion doesn't poison radius measurement
- Previously gave 14 km radii, difficult to reconcile with qLMXB radii, now in agreement
- Systematic uncertainties difficult here as well

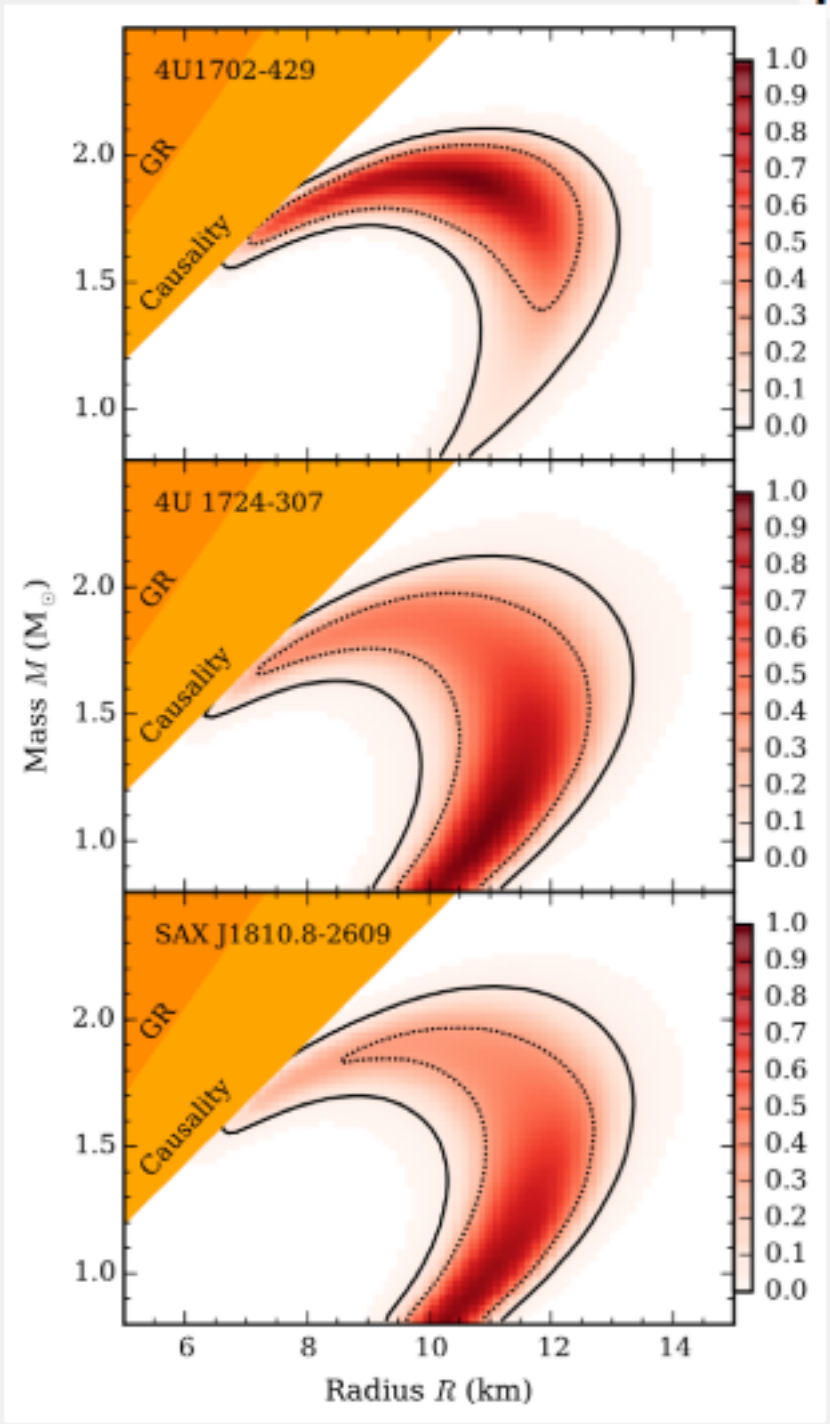

Nättilä et al. (2016)

Presence of Phase Transitions Above Saturation

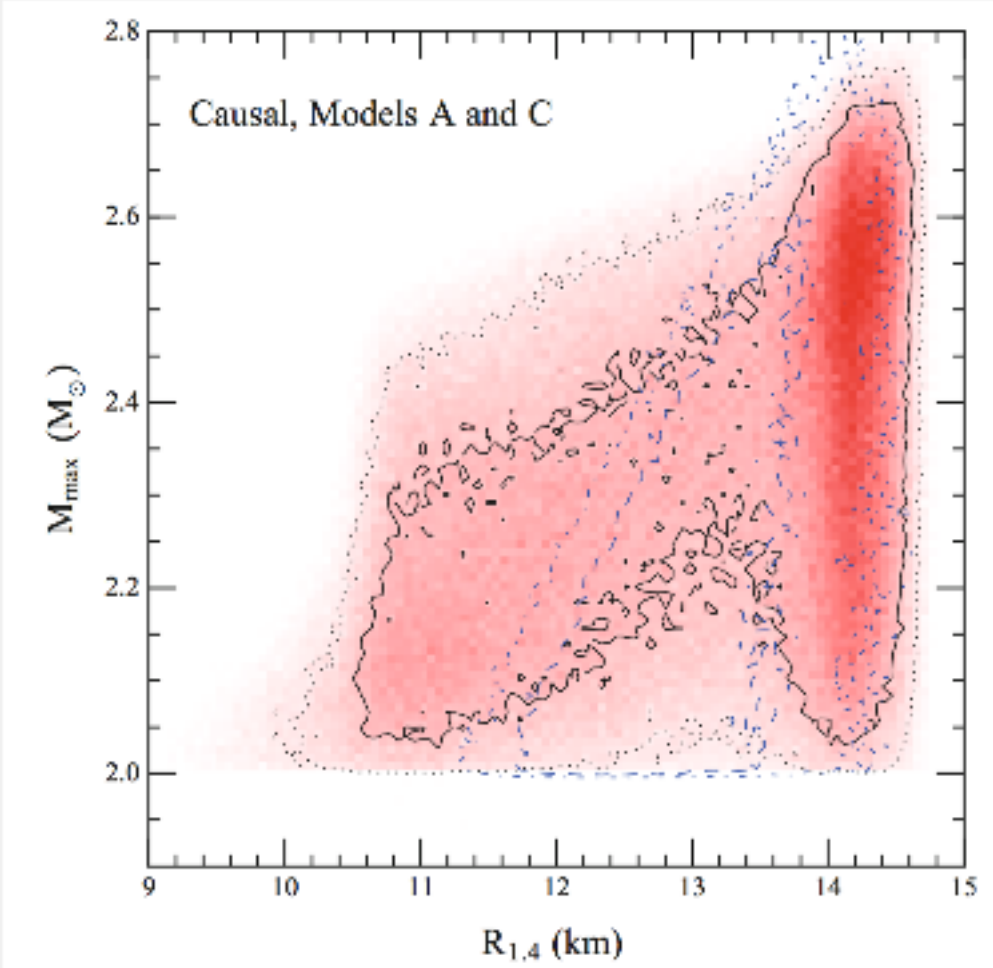

Steiner, Lattimer, and Brown (2016)

- Choice of prior distribution has a significant affect on radius, even after fixing data
- The principal difference here is the possible presence of a phase transition just above saturation
- Some results from chiral effective theory and heavy-ion collisions suggest phase transitions only at higher densities

  But uncertainty quantification is difficult in these cases

M-R and EOS results

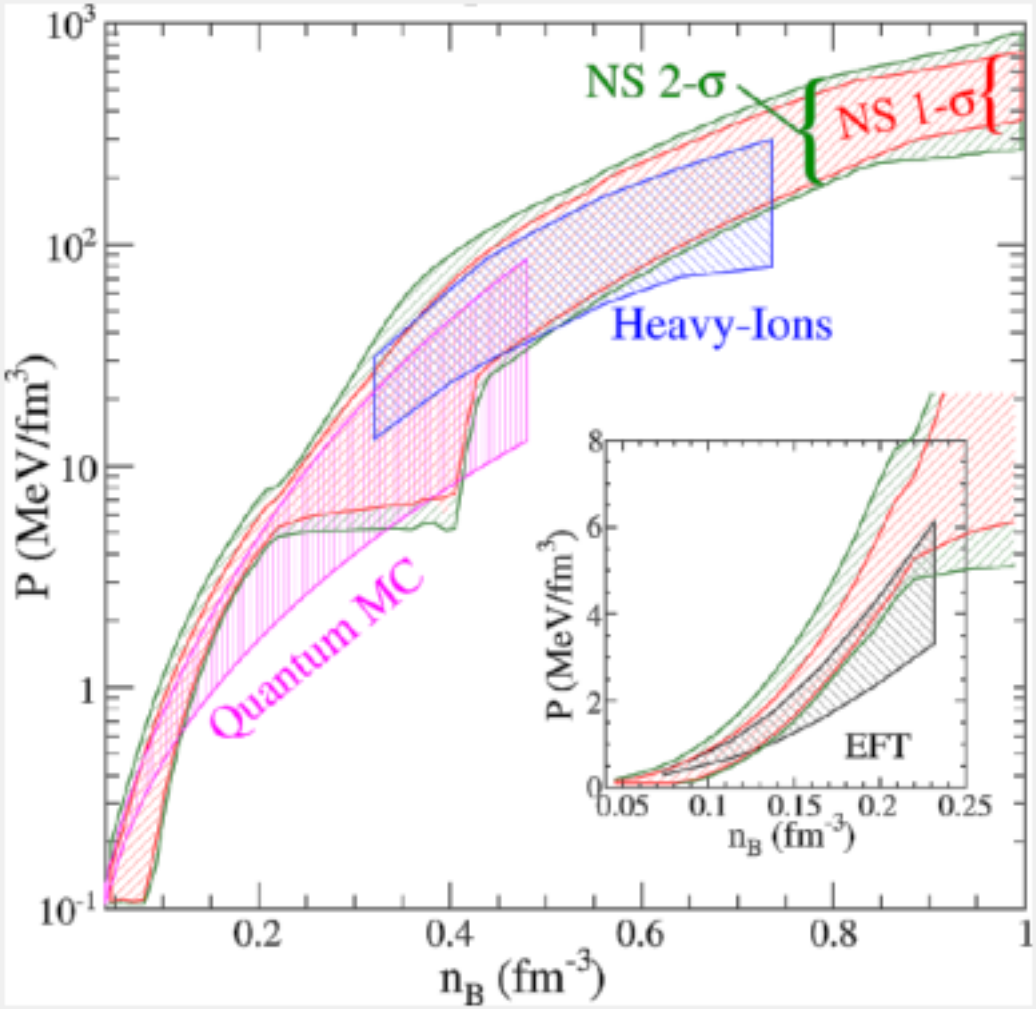

Steiner, Lattimer, and Brown (2013)

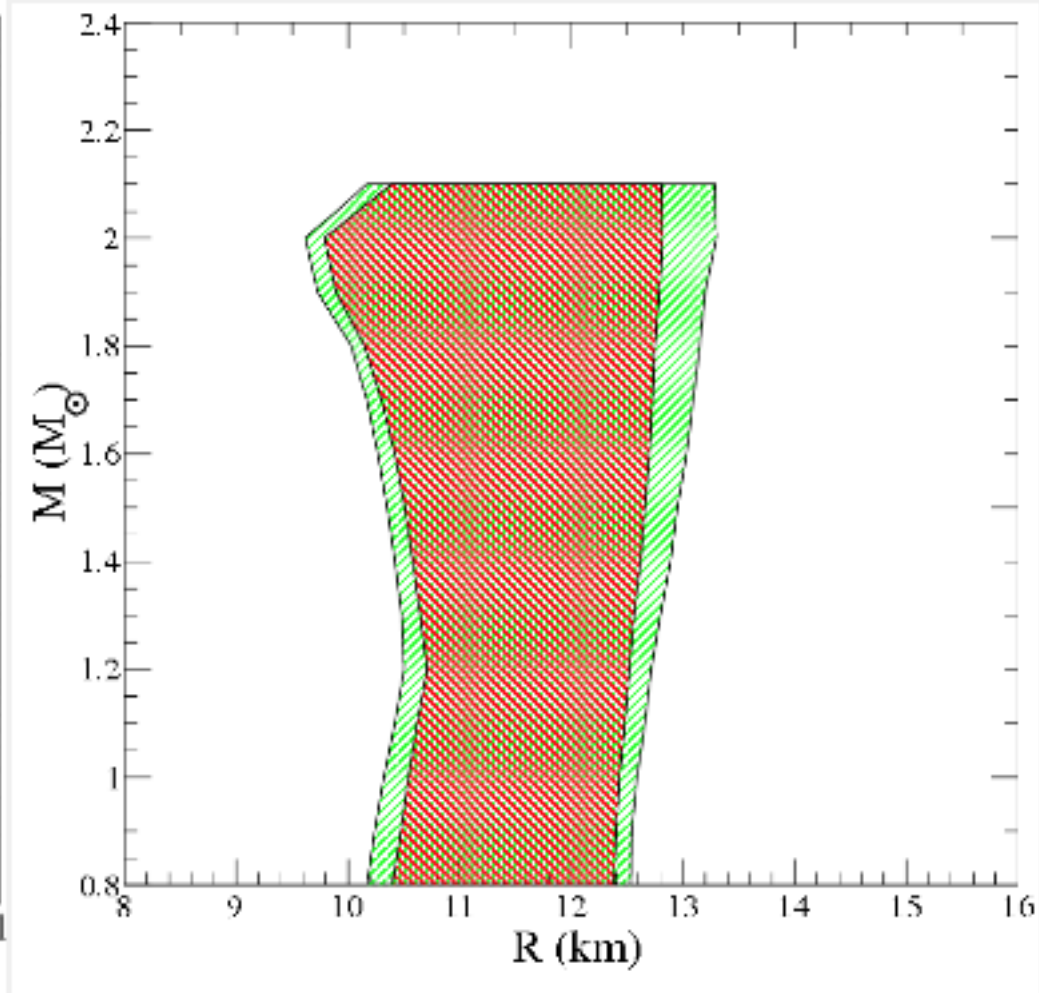

Steiner, Lattimer, and Brown (2013)

- Choose to allow phase transitions below twice the nuclear saturation density
- Ensure bounds enclose results from different models
- 10 – 13 km radii
- EOS consistent with nuclear physics constraints
- From 2013, but this result still stands

M-R and EOS results

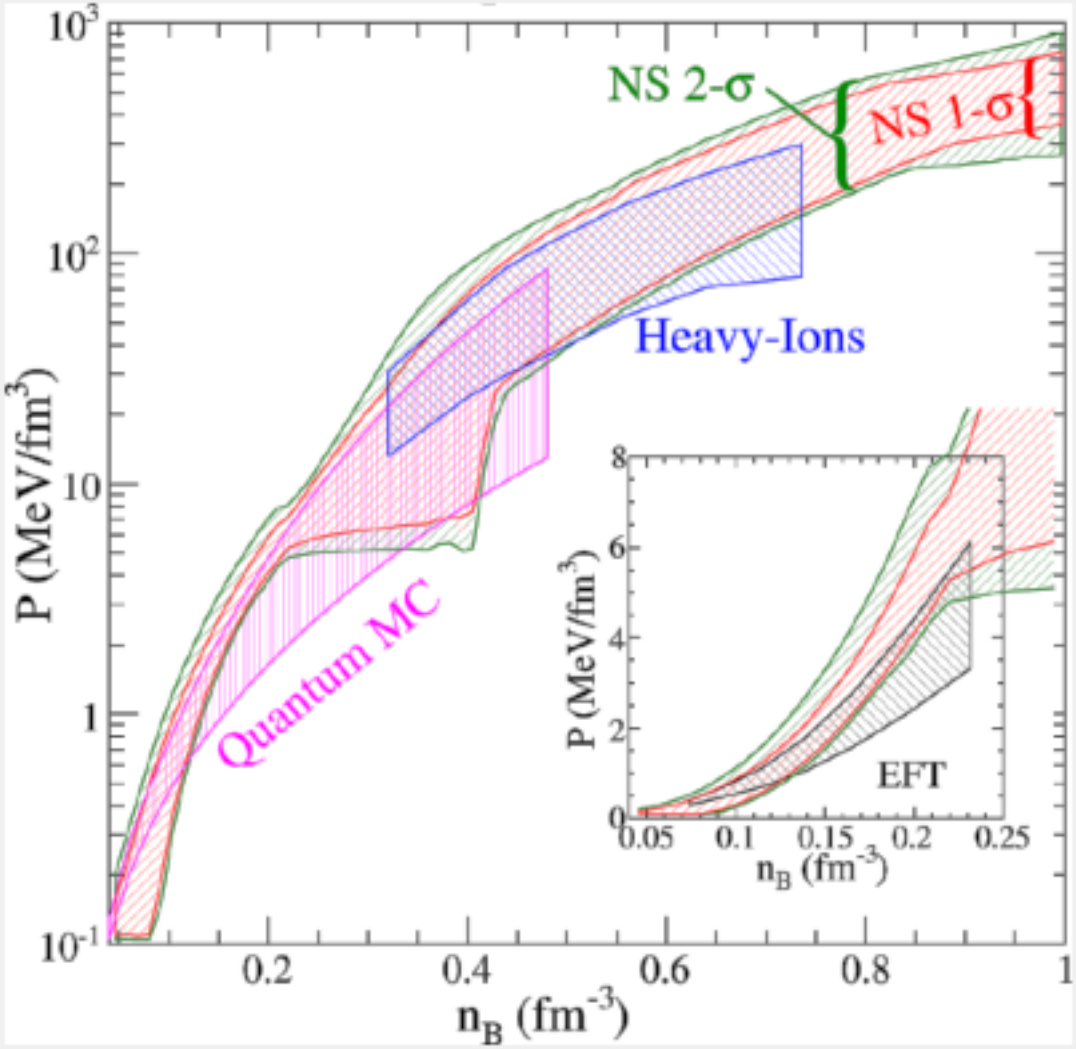

Steiner, Lattimer, and Brown (2013)

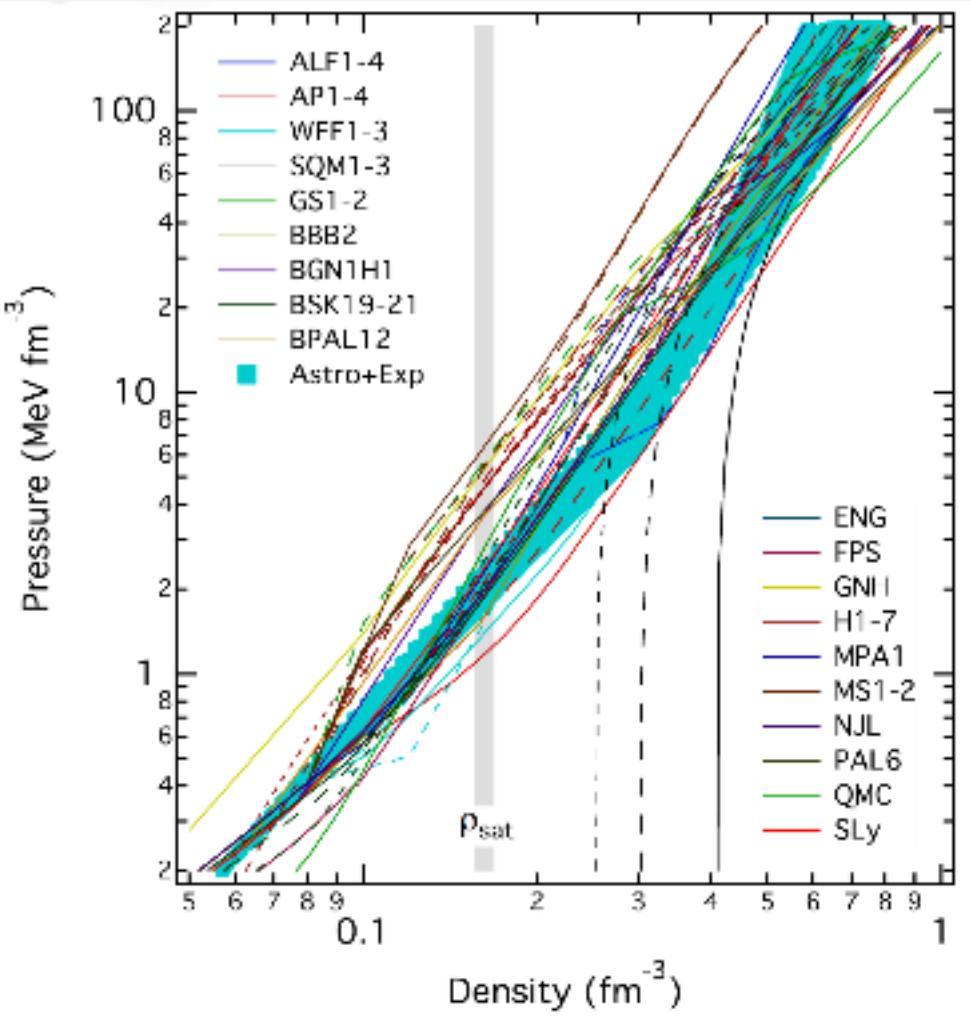

Özel and Freire (2016)

- Choose to allow phase transitions below twice the nuclear saturation density

  Some authors disallow these, and thus obtain tighter constraints

  Özel et al. obtain smaller radii, but without strong phase transitions at low densities this will lead to smaller Bayes factors

I and λ results

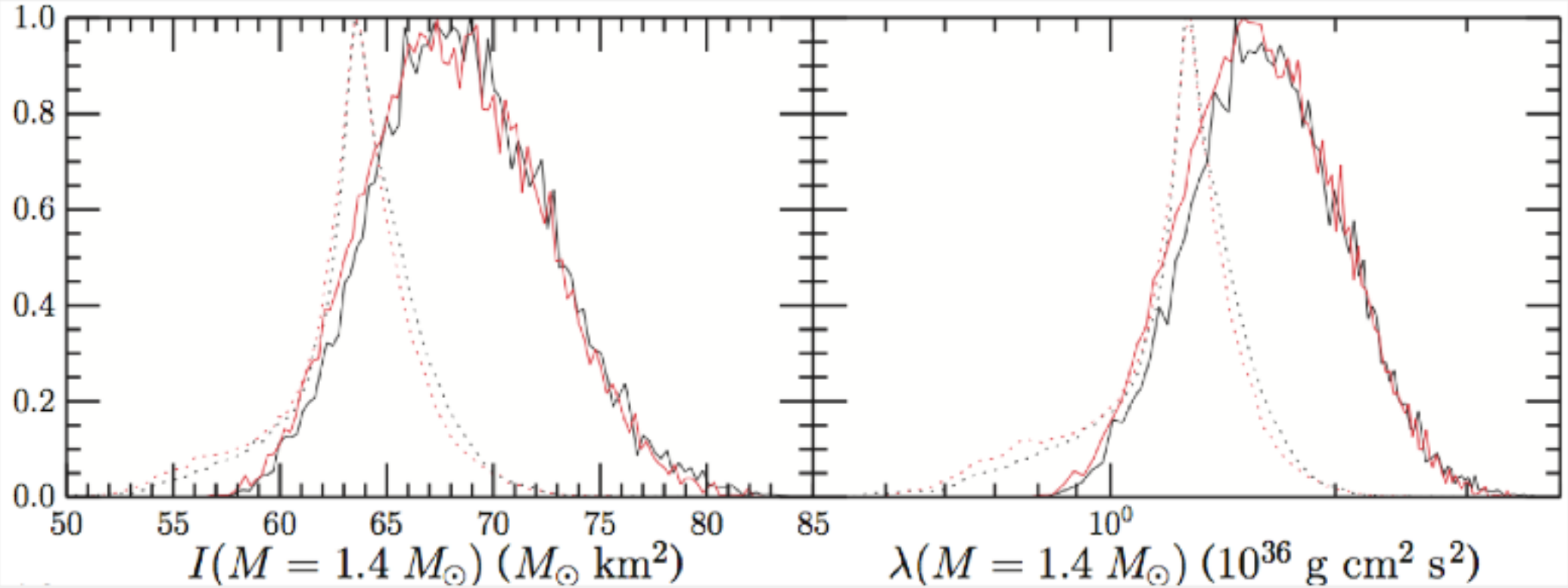

Steiner et al. (2015)

- Predict moments of inertia and tidal deformabilities
- Tidal deformability is like a tidal polarizability for gravitational fields
- Potentially exciting comparison with LIGO observations
- Note again the strong model dependence
- These plots do not include several astrophysical systematics

Correlations and/or "Universal Relations"

- Take advantage of relationships between observables
- Quantification of our current theoretical ignorance

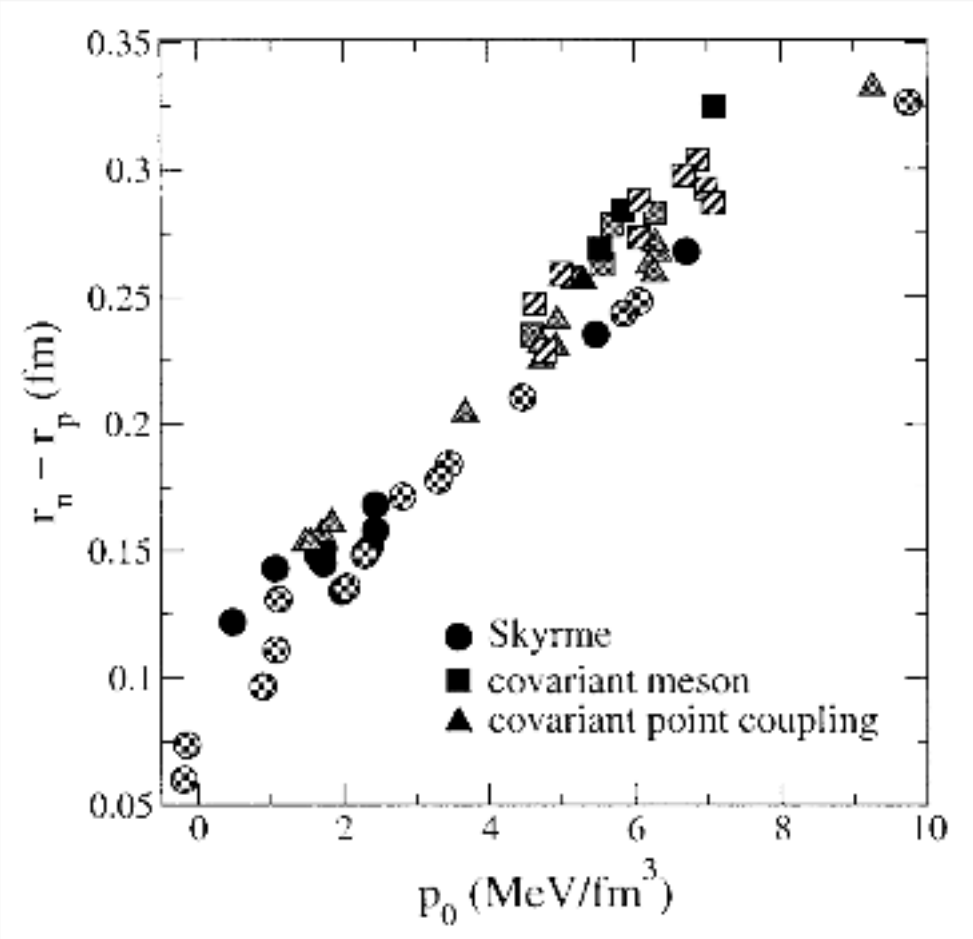

Furnstahl (2002)
(p_0 is related to L)

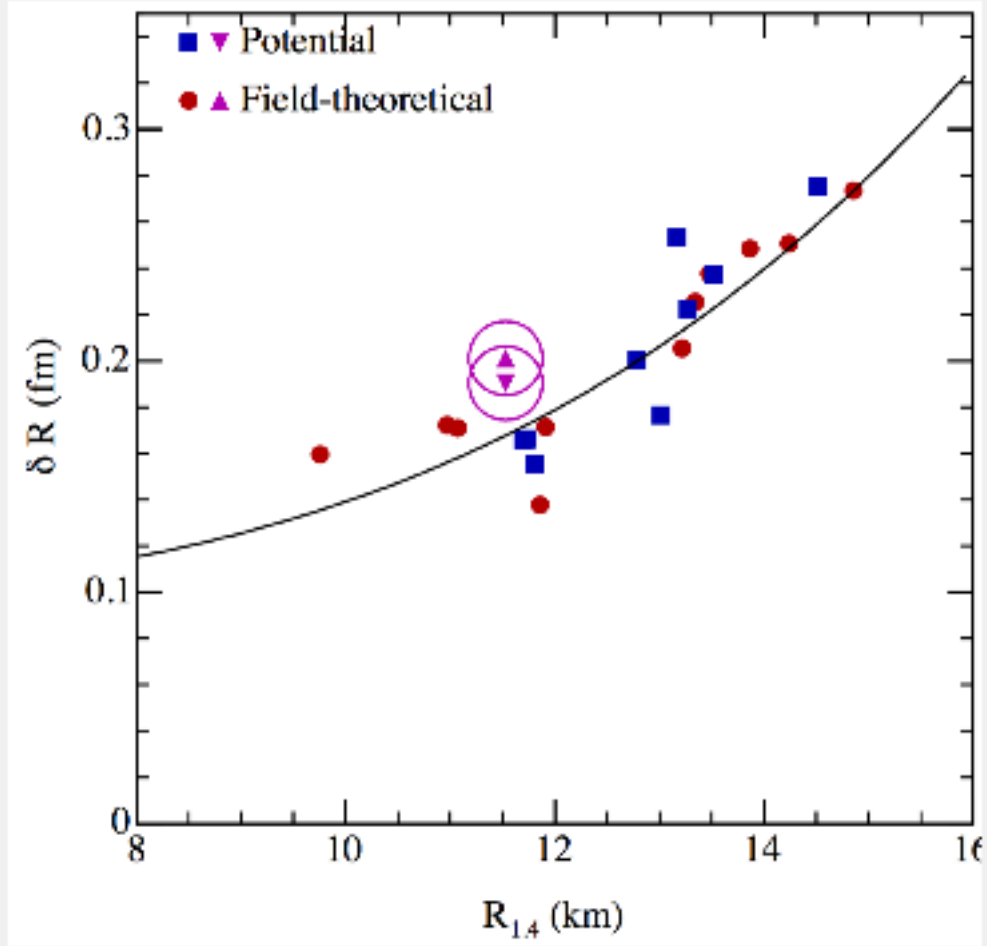

Steiner et al. (2005)
based on Horowitz and Piekarewicz (2001)

- 2-3 models and a dozen parameterizations (not optimally chosen) for each model
- Plots like this can be dangerous!

Quantifying Correlations

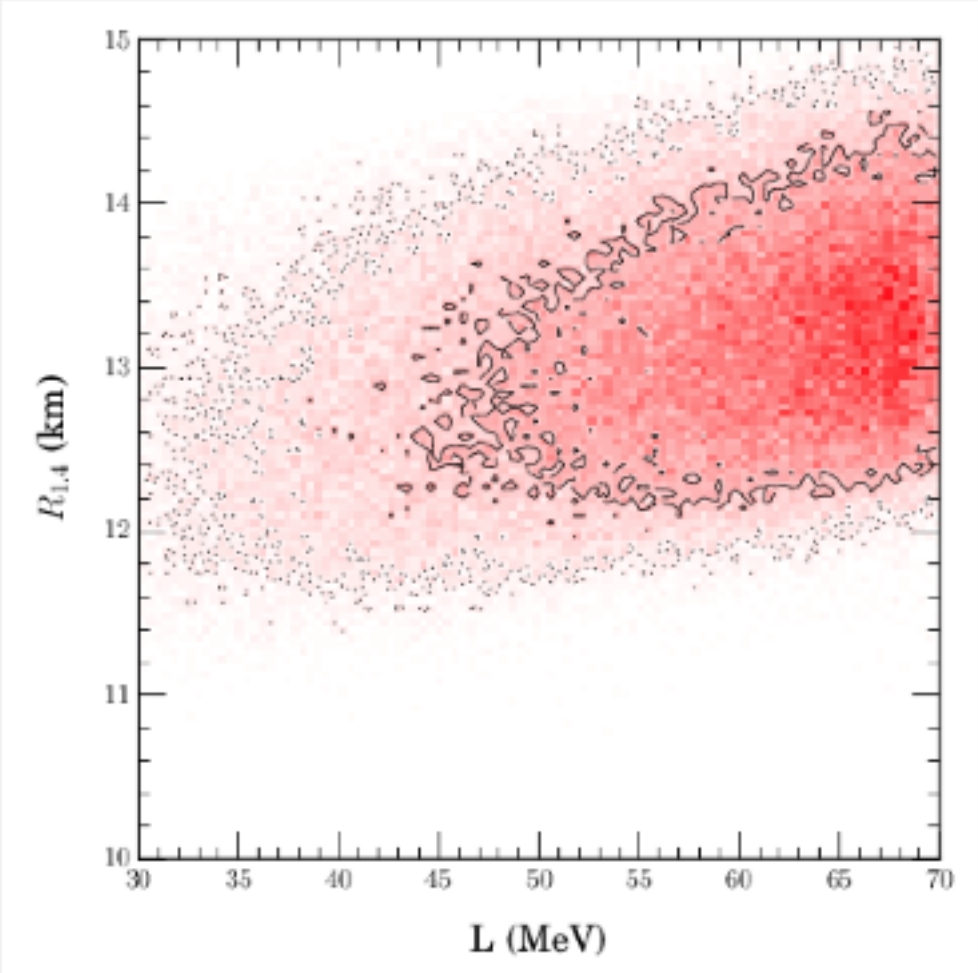

line-segments in $\log P - \log \varepsilon$

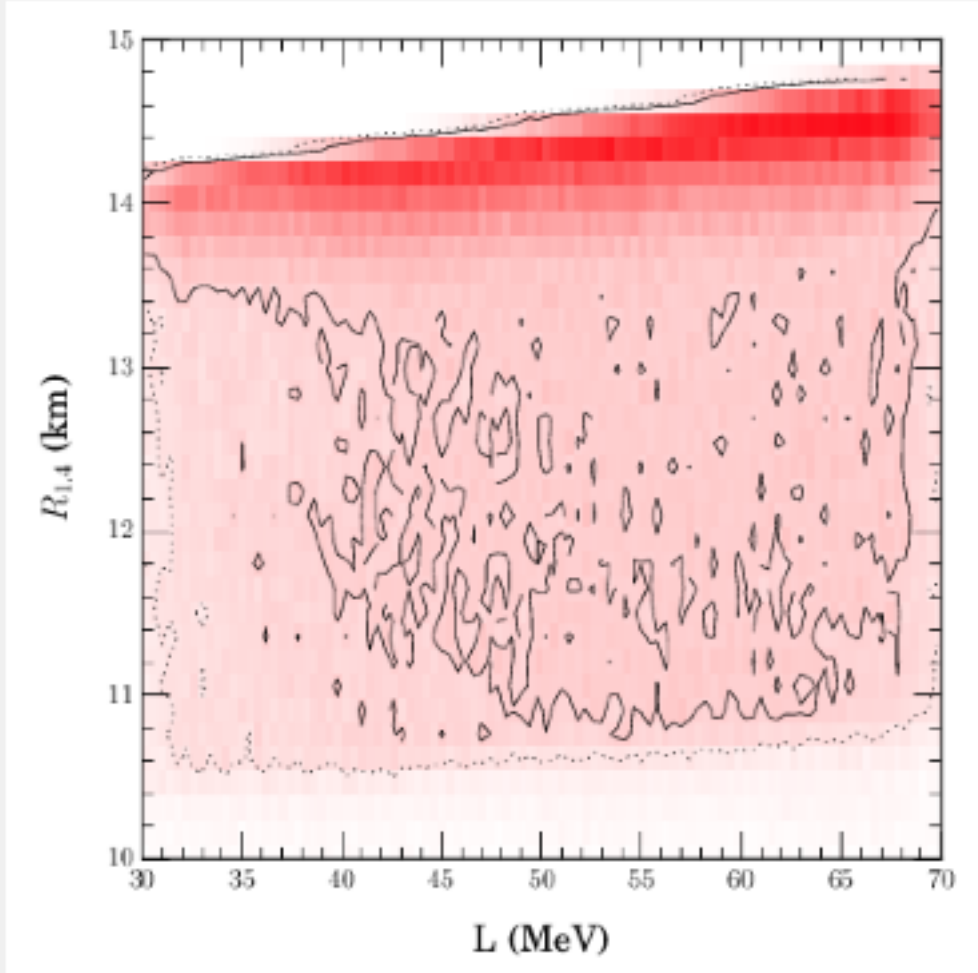

line-segments in $P - \varepsilon$

Based on Steiner, Lattimer, and Brown (2016)

- Shown are probability distributions with no radius data
- Replace dozens of points with millions of points
- The correlation between L and $R_{1.4}$ is strongly dependent on model assumptions

  Phase transitions potentially break the correlation

Correlations without Radius Information

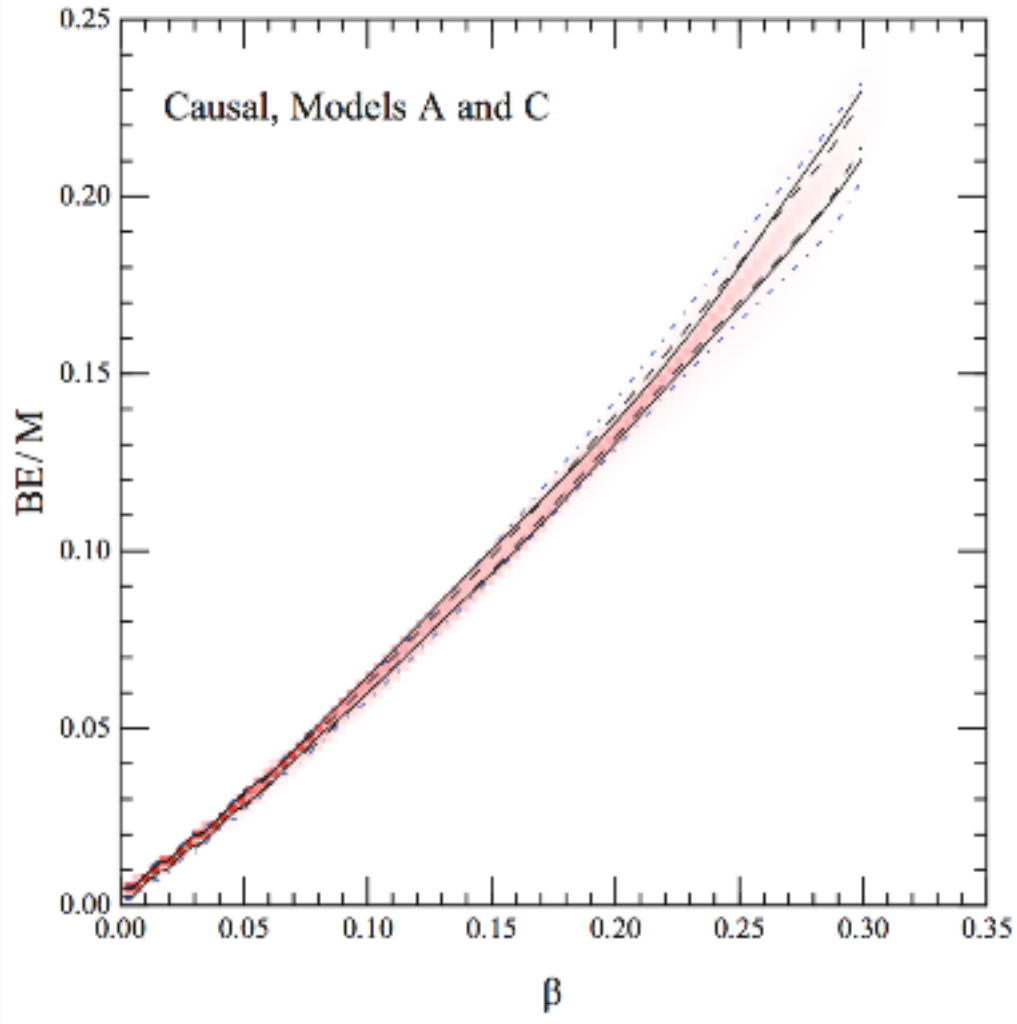

Steiner, Lattimer, and Brown (2016)

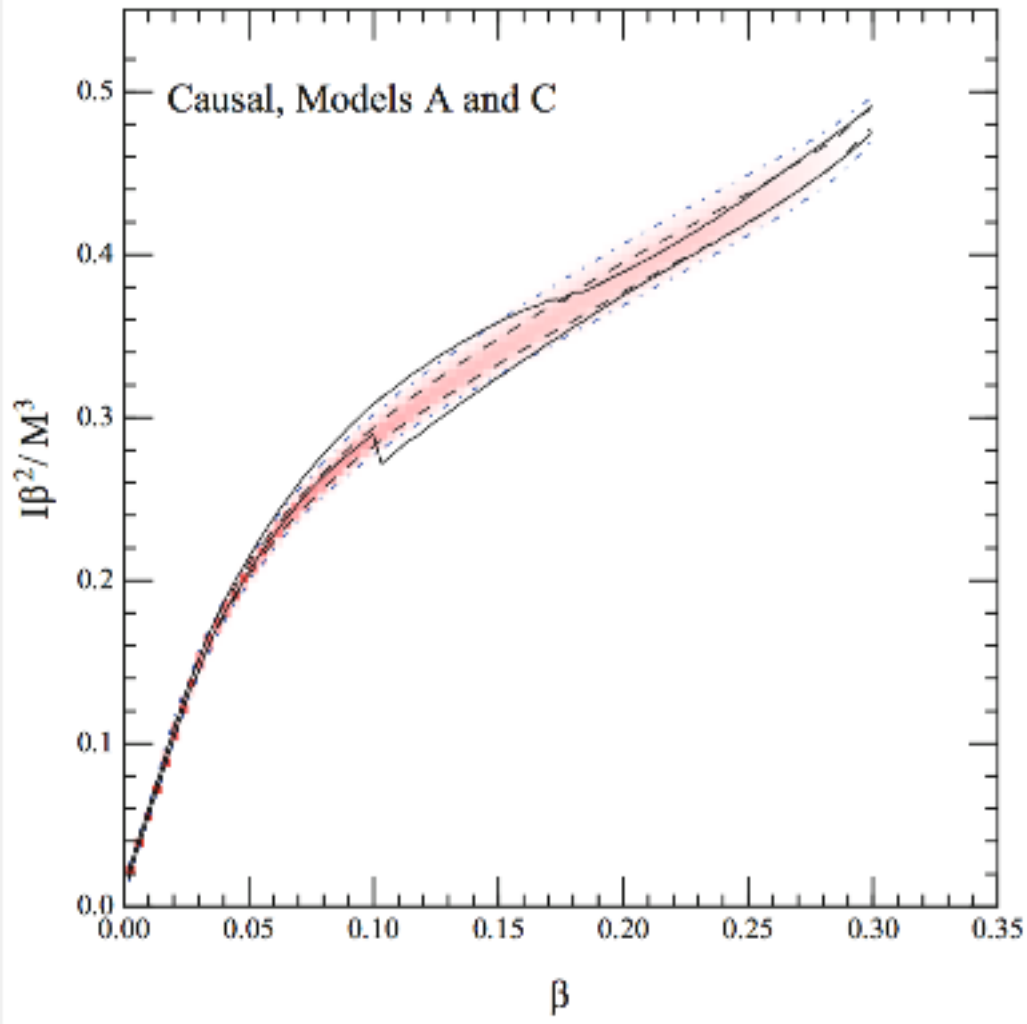

Steiner, Lattimer, and Brown (2016)

- Compactness strongly correlated with binding energy and moment of inertia
- Smaller dependence on the presence of phase transitions

Correlations without Radius Information - II

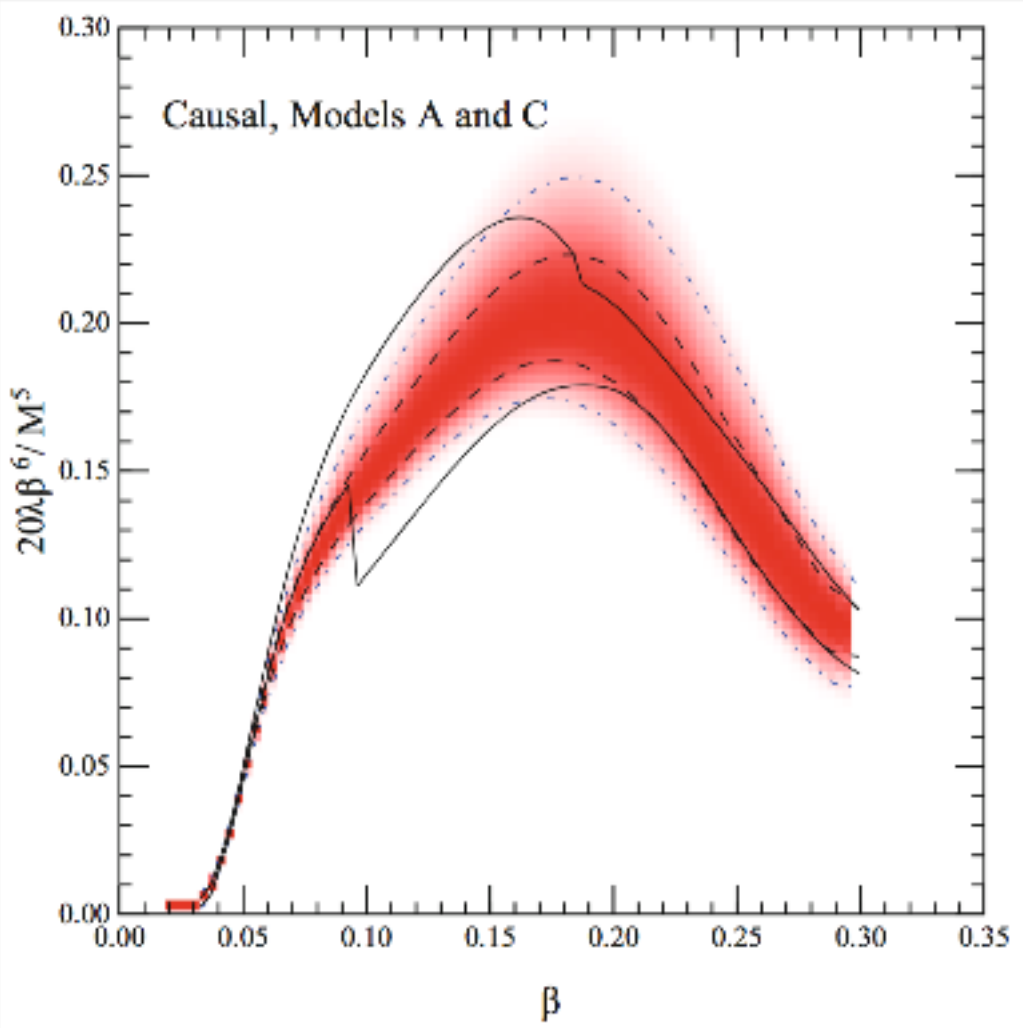

Steiner, Lattimer, and Brown (2016)

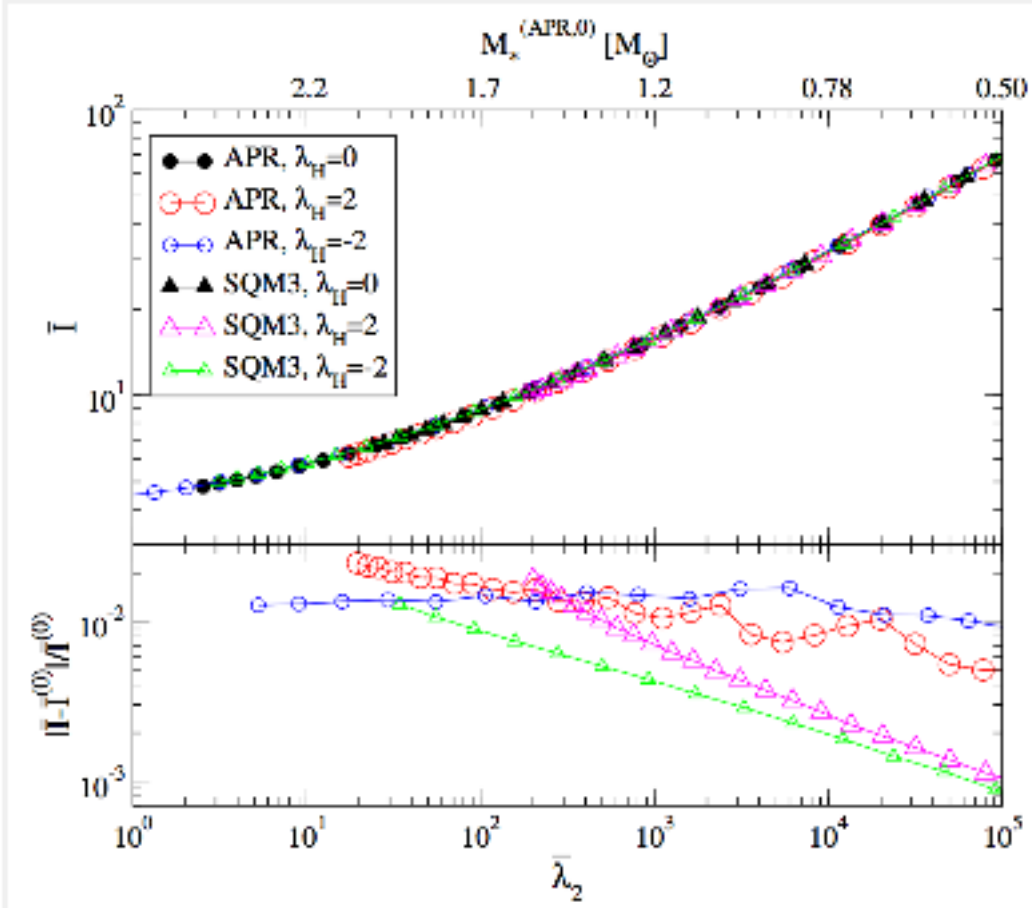

Yagi and Yunes (2015)

- Compactness weakly correlated with tidal deformability
- Tidal deformability very strongly correlated with moment of inertia

EOS for astrophysical simulations

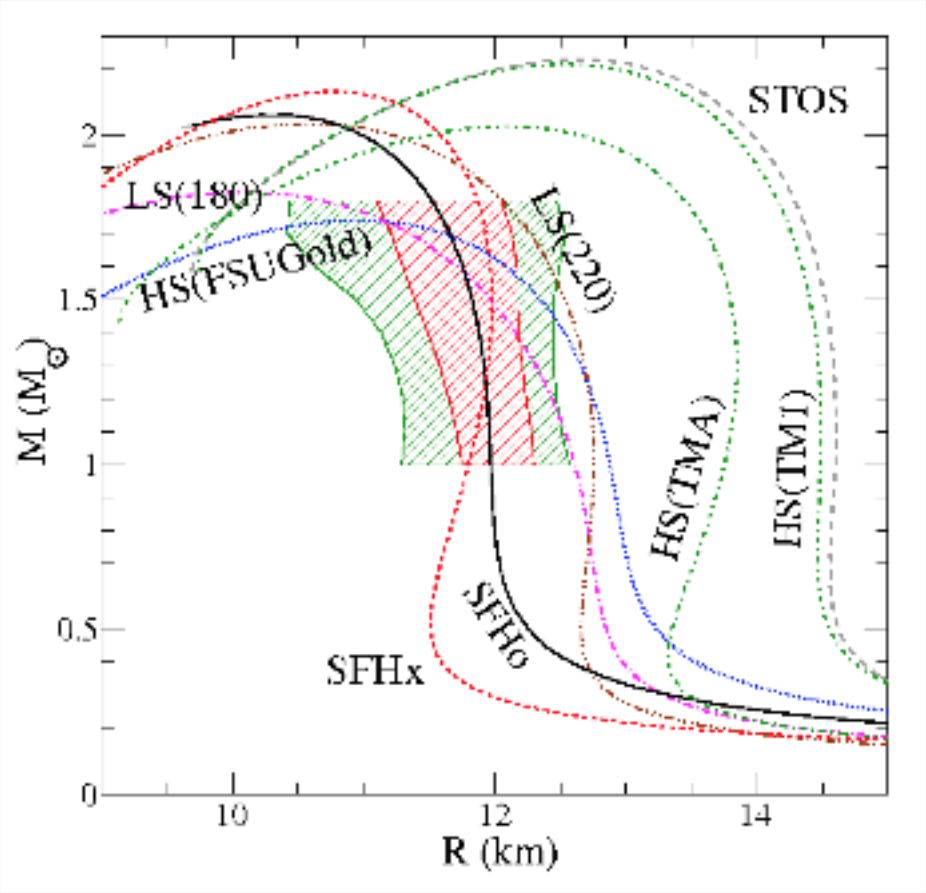

Steiner, Hempel and Fischer (2013)

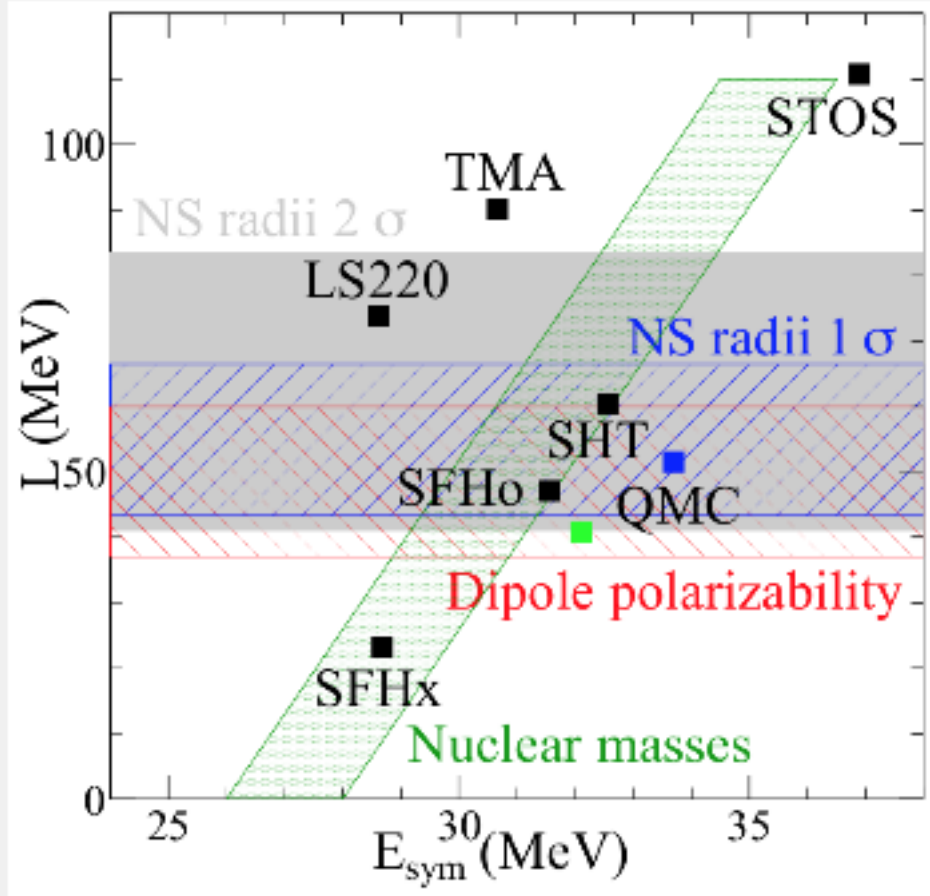

Based on Steiner, Hempel and Fischer (2013)

- Limited number of EOS tables (Y_e, n_B, T) which satisfy $M - R$ constraints and the $S - L$ correlation
- Current EOS uncertainties too small to explain explosion
- Many simulation properties are weakly correlated with the symmetry energy

Mergers and the r-process

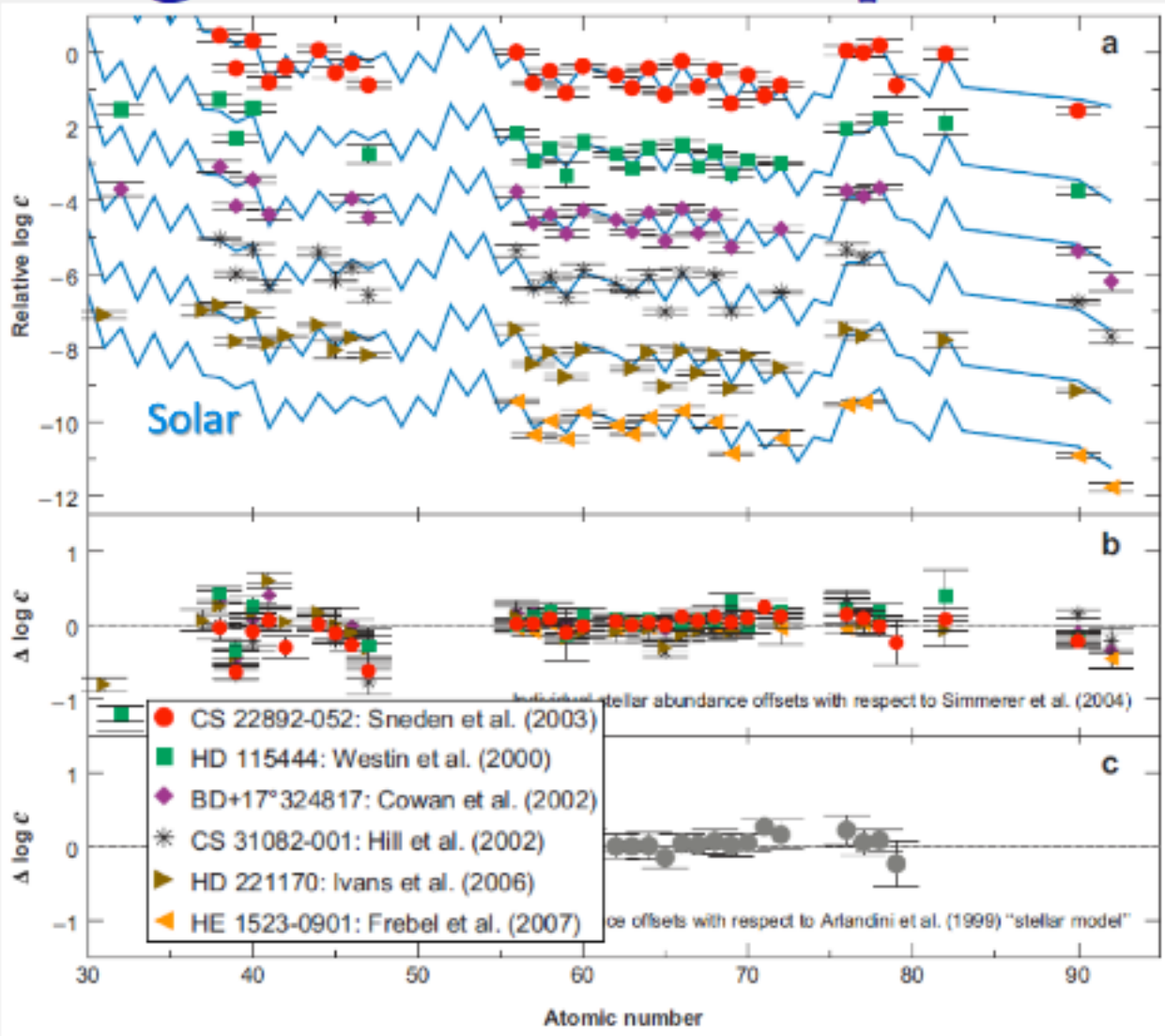

- r-process nuclei observed in stars is universal: same pattern from event to event
- May occur in neutron star mergers, but is it universal?

Mergers and the r-process

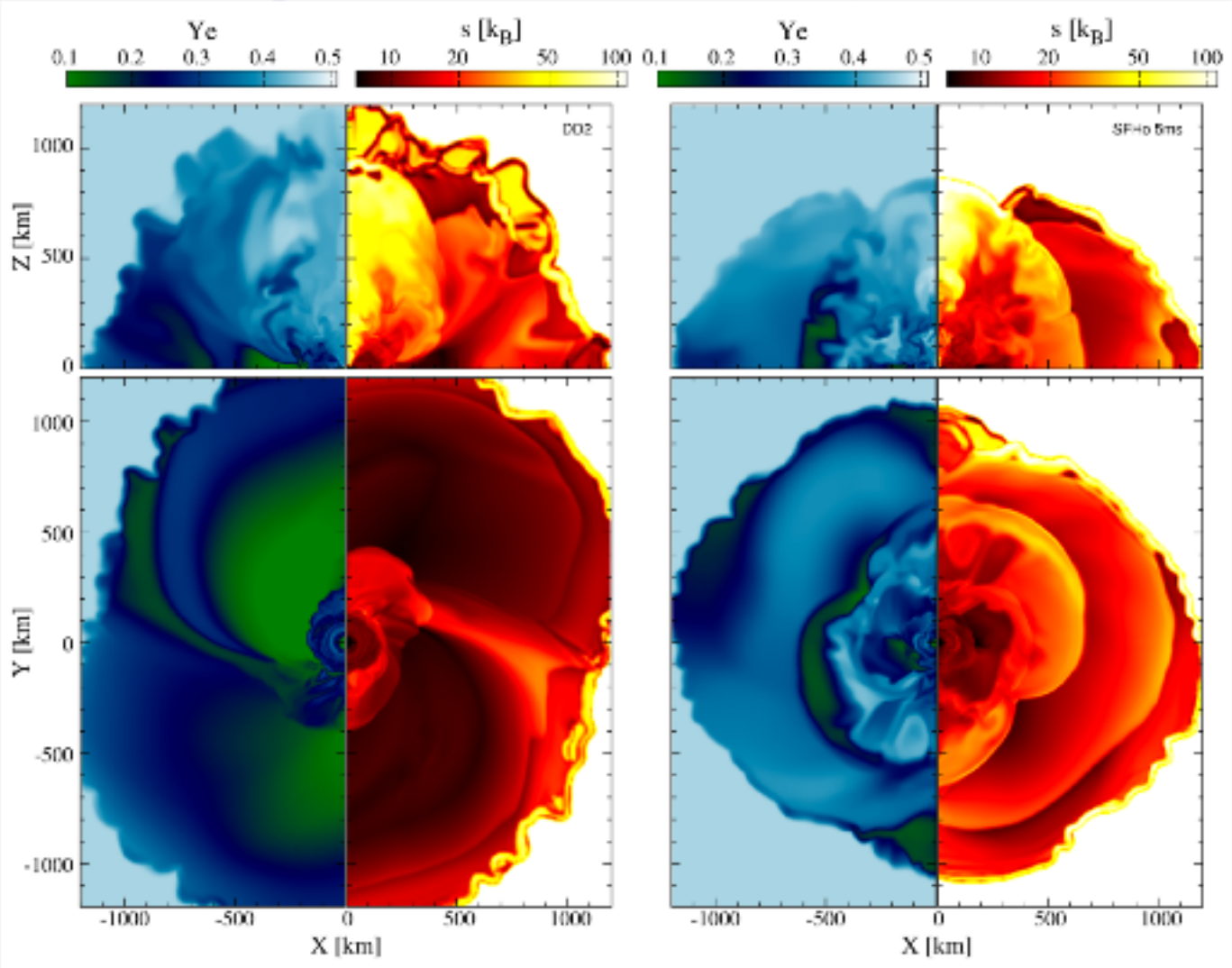

Sekguchi et al. (2015), DD2 (large radii) on left and SFHo (small radii) on right

- Small radii lead to higher Y_e and more universal r-process production
- Smaller radii also lead to larger amounts of ejected r-process material

Summary

- Difficult data analysis problem
  Bayesian inference is an excellent solution
- Phase transitions, especially at low densities, are an issue
  Need to figure out how to push to higher densities in theory and experiment
- Attempt to be as complete as possible
- Neutron star radii: 10 to 13 km
- From Steiner et al. (2015)
  - Central baryon densities between 4.7 to 7.7 times the saturation density
  - $I_{1.4}$ between 57 and 77 $\mathrm{M}_\odot$ km^2
  - $\lambda_{1.4}$ between 0.73 and 2.6×10^{36} $\mathrm{g\ cm^2\ s^2}$
  - Crust thickness (1.4) between 0.60 and 1.26 km
- New correlations β vs. BE/M, β vs. $I\beta^2/M^3$, and β vs. $\lambda\beta^6/M^5$

- Need new data! LOFT!

Danger of Extrapolation

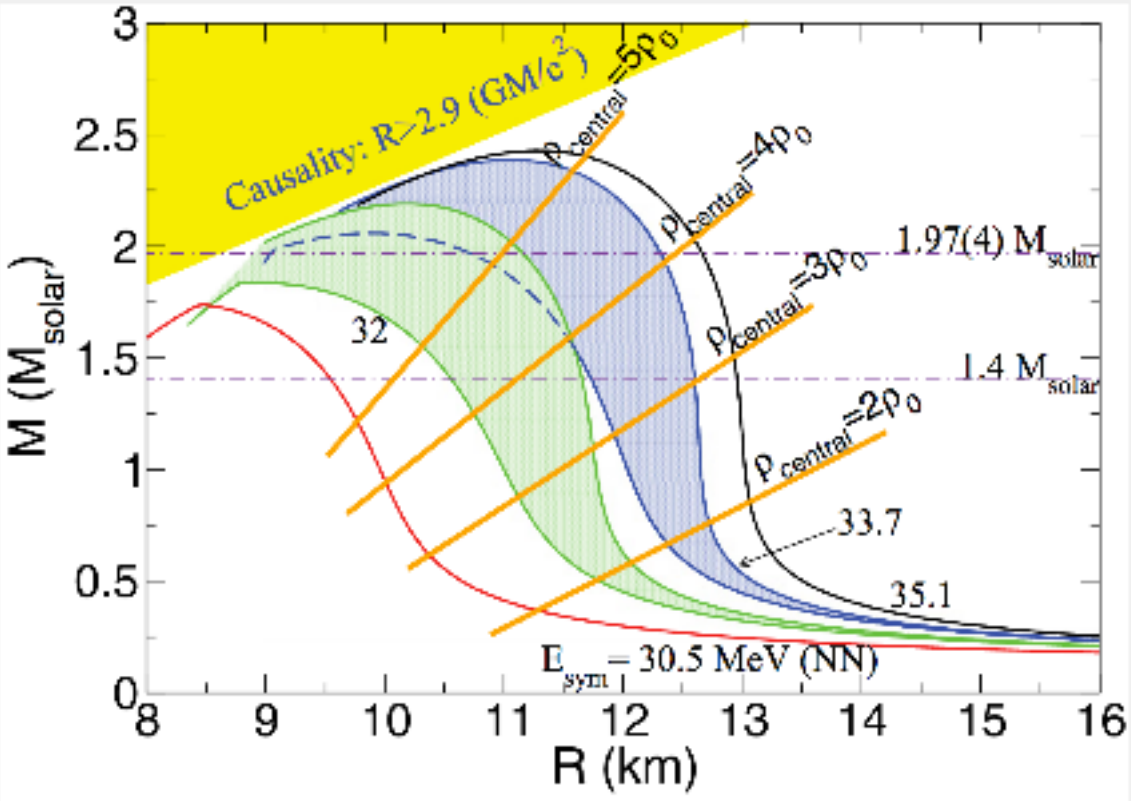

Gandolfi et al. (2012)

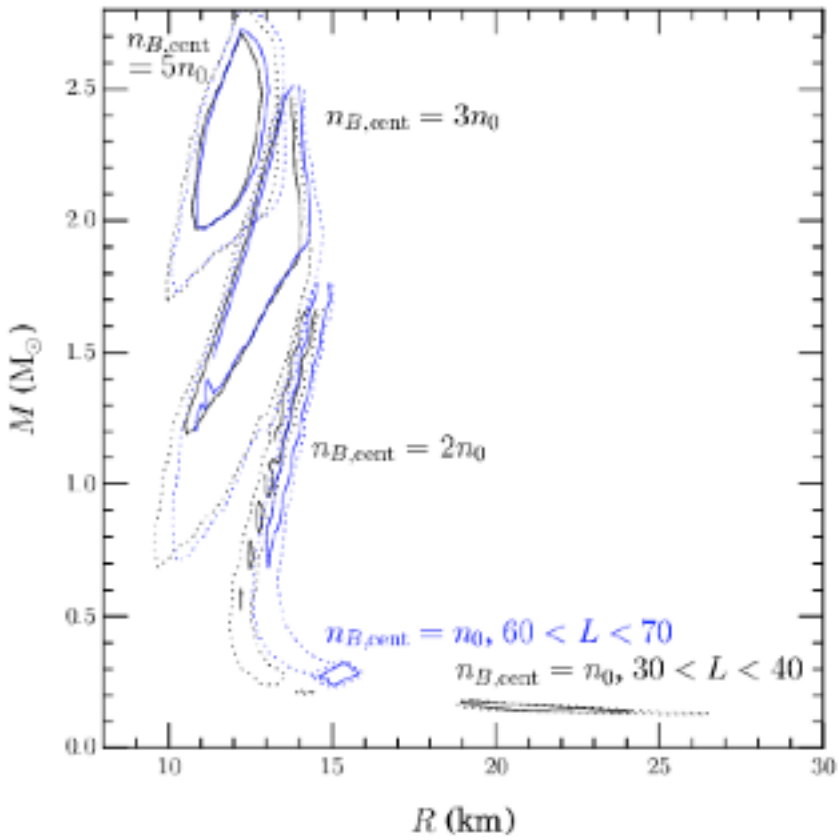

Model C from Steiner et al. (2016)

- Extrapolation gives an overly simplistic impression of the nature of dense matter

Extrapolation: The Tail Wags the Dog

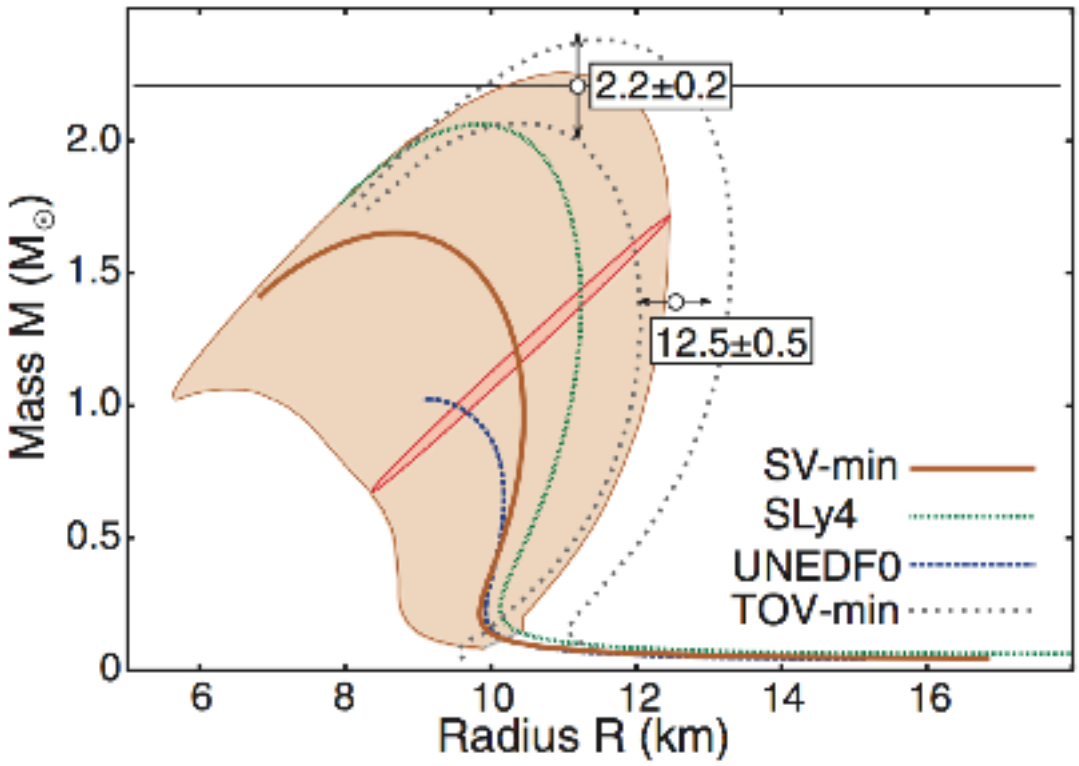

FIG. 2. (Color online) Mass-radius relation of SLy4 [1], UNEDF0 [22] and SV-min [24]. The uncertainty band for SV-min is shown. This band is estimated by calculating the covariance ellipsoid for the mass M and the radius R at each point of the SV-min curve as indicated by the ellipsoid. Also depicted (dotted lines) are uncertainty limits for TOV-min.

Erler et al. (2013)

- Many works extrapolate models of the nucleon-nucleon interaction up to very large densities
- Bayesian inference can alleviate this problem
- Arrange prior distribution to properly reweigh the dog and its tail
- Important issue when fitting disparate data sets to one model
- Related to "overfitting"

Pulsar Glitch Mechanism

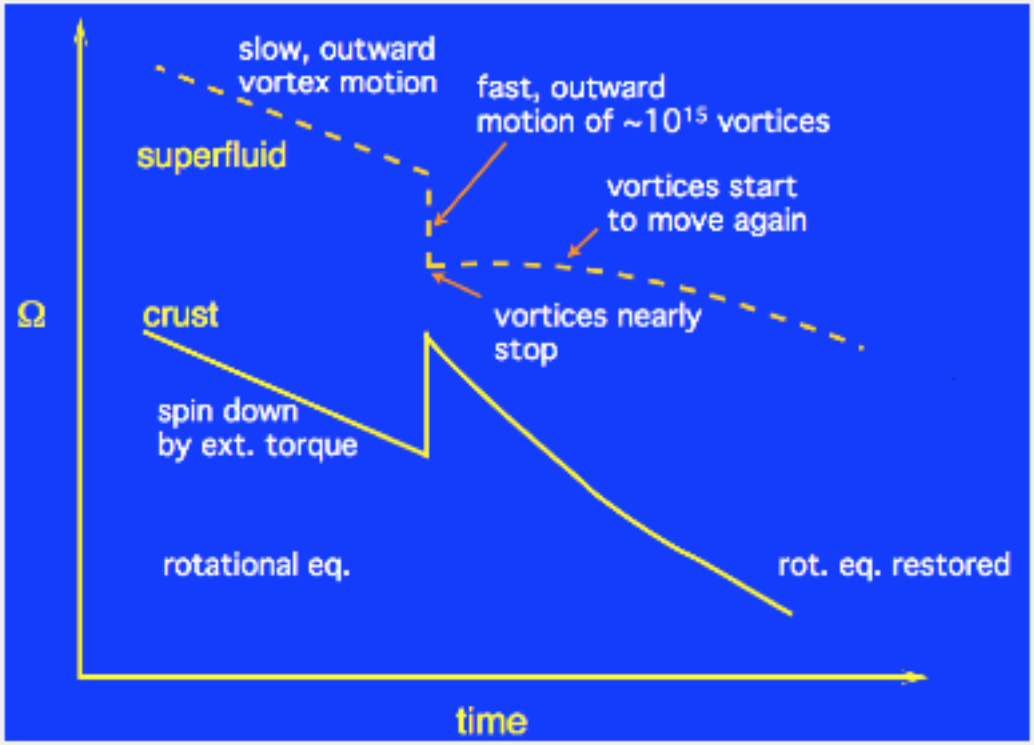

Picture from B. Link

- Superfluid component, decoupled from rotation at the surface
- Natural to associate the superfluid component with the superfluid neutrons in the crust
- What is the mechanism for the sudden change?

- Superfluid vortices pinned to the lattice
- Neutron star spins down, vortices bend creating tension, eventually they must shift lattice sites
- Quasi-free neutrons are entrained with the lattice

Chamel 2012, Chamel et al. 2013

Is There Enough Superfluid in the Crust?

- We require 1.6% of I to explain glitches in Vela
  Link, Epstein, and Lattimer (1999)

- Entrainment: 75-85% of otherwise superfluid neutrons 'connected' to the lattice
  N. Chamel (2012)

- Current M and R observations suggest there is not enough I in the crust
  See Andersson et al. (2012)

- Unless the systematics force much larger neutron star radii and P_t and L are large

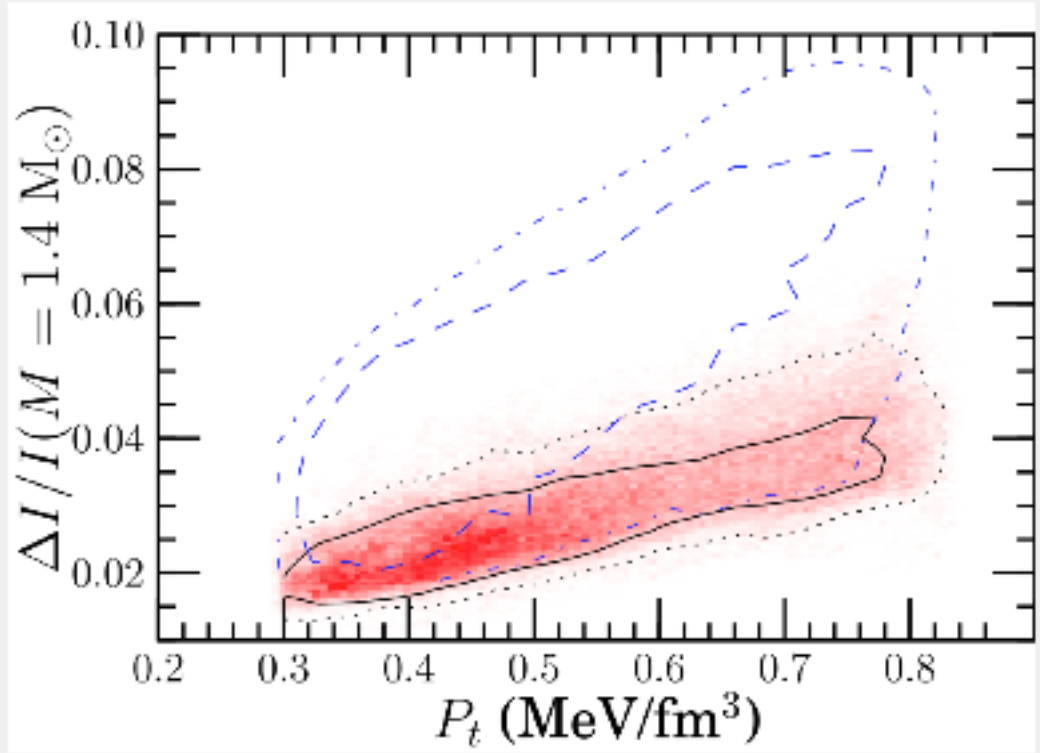

Steiner et al. (2014); black and red are with M & R observations, blue contours are with $I = 70\ \mathrm{M}_\odot\ \mathrm{km}^2$

Crust Thickness and Pasta

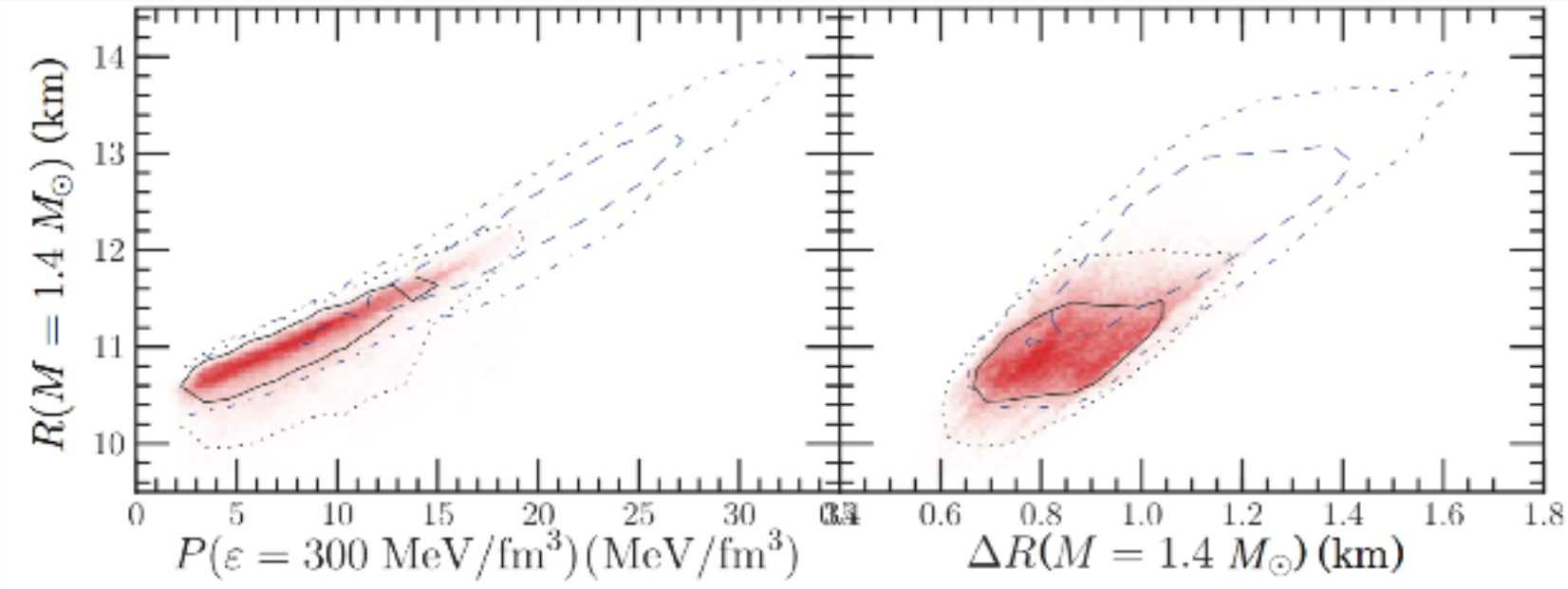

Steiner, Gandolfi, Fattoyev, and Newton (2015)

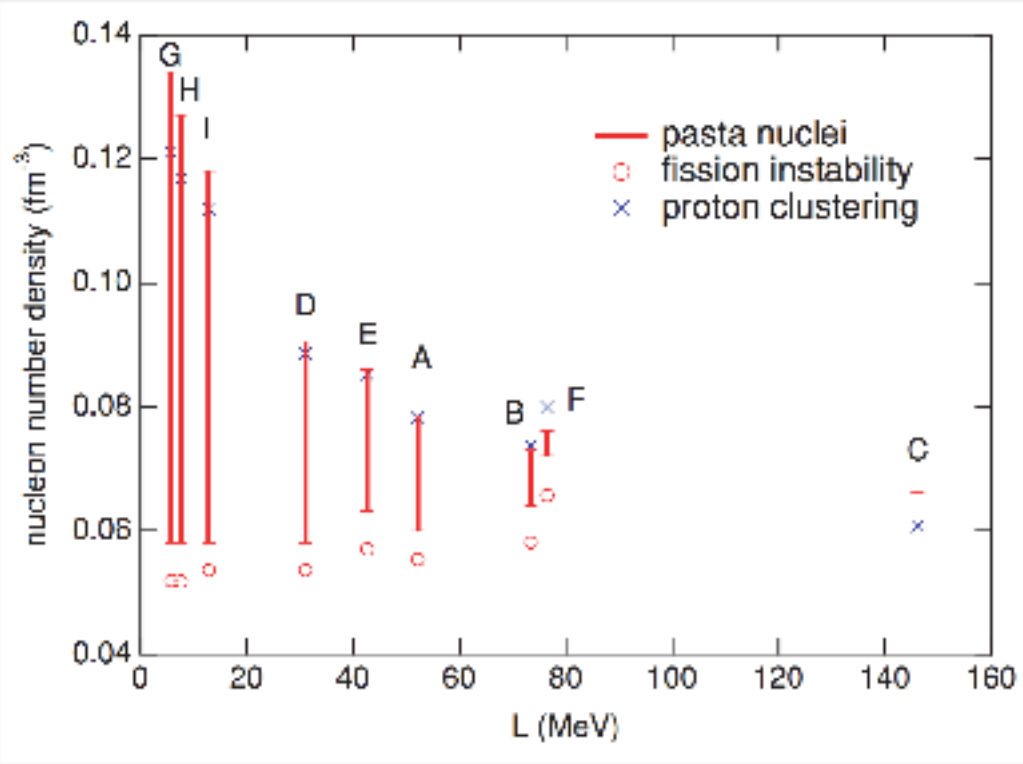

Oyamatsu and Iida (2007)

- L connected to crust thickness and the extent of the nuclear pasta

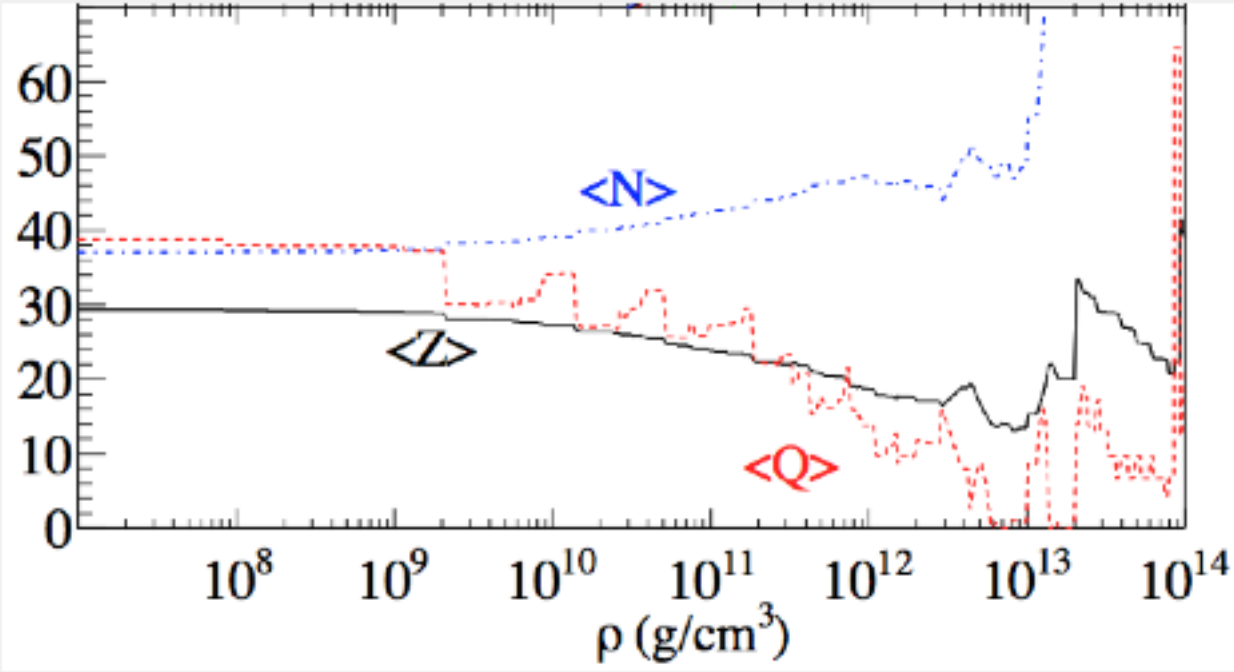

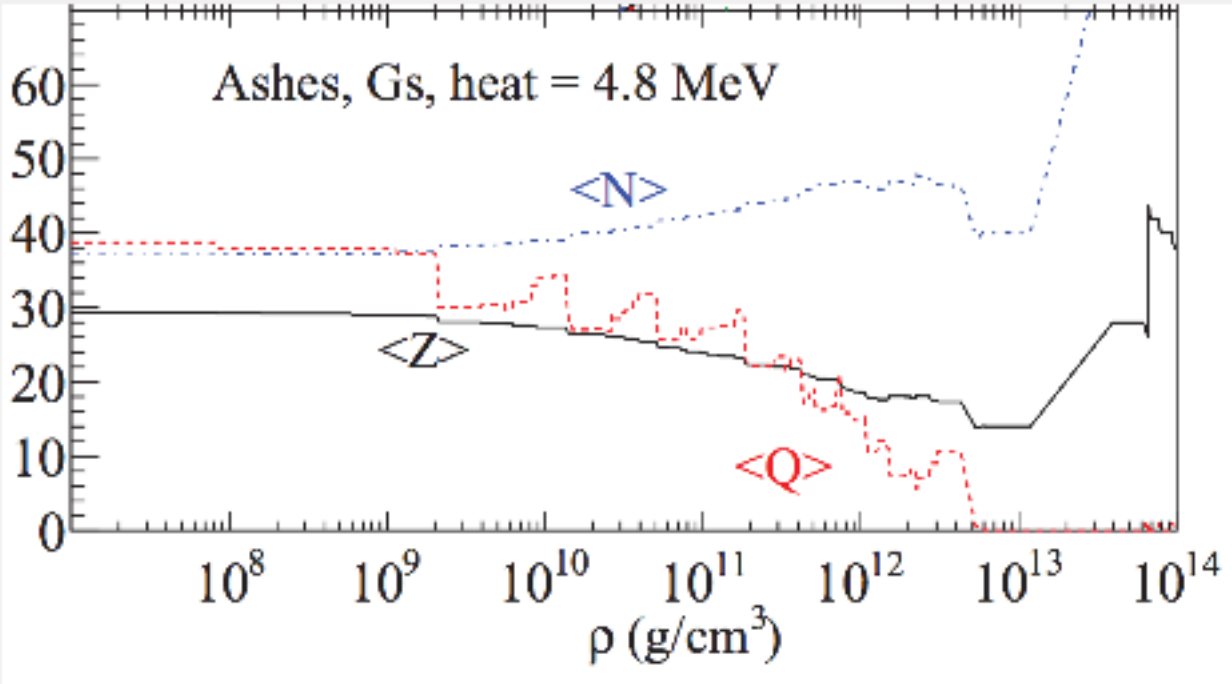

Steiner (2012)

Deep Crustal Heating

- L connected to the amount of heating in an accreting neutron star crust

Stellar Evolution

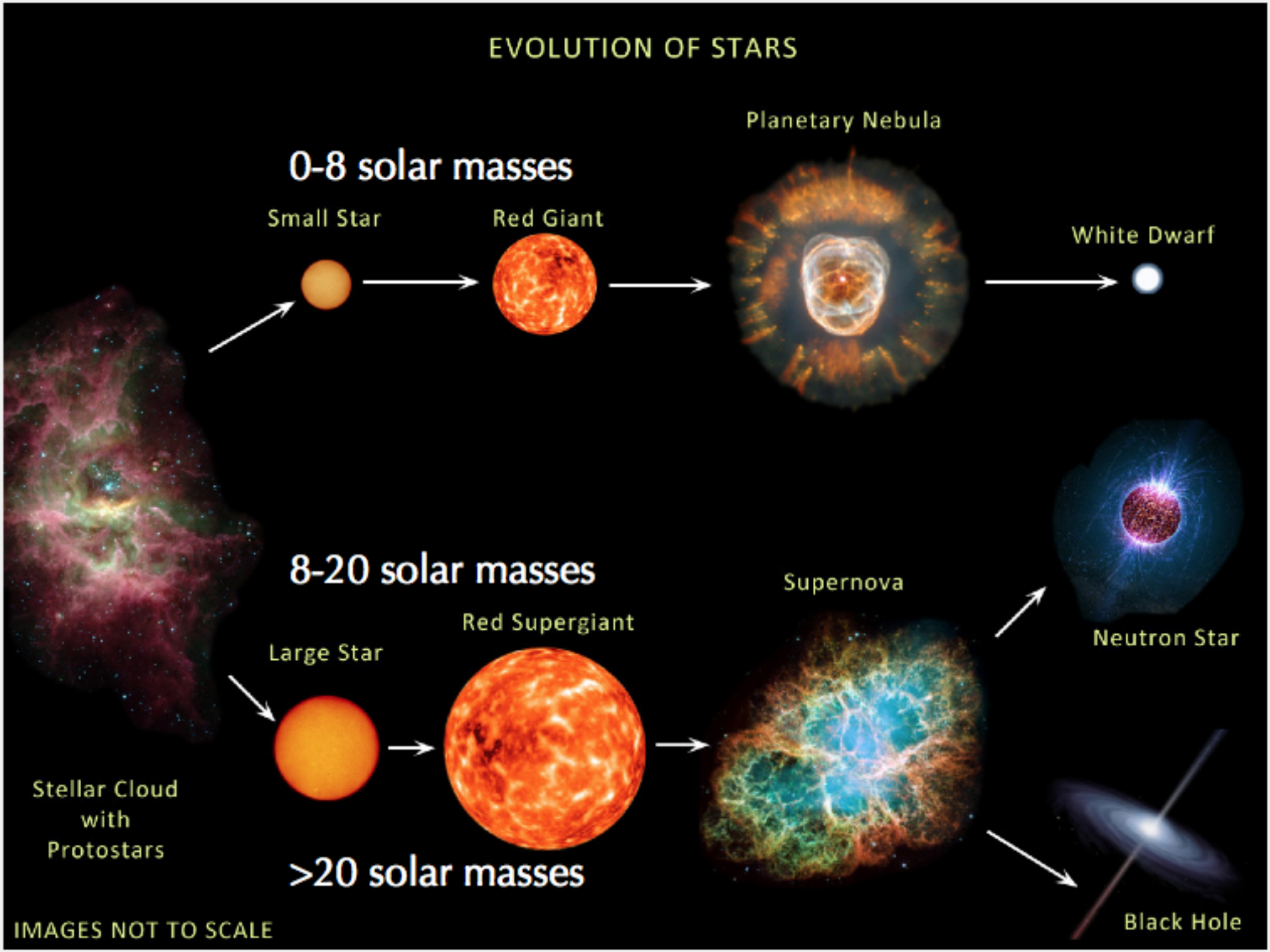

Structure of Matter in the Neutron Star Crust

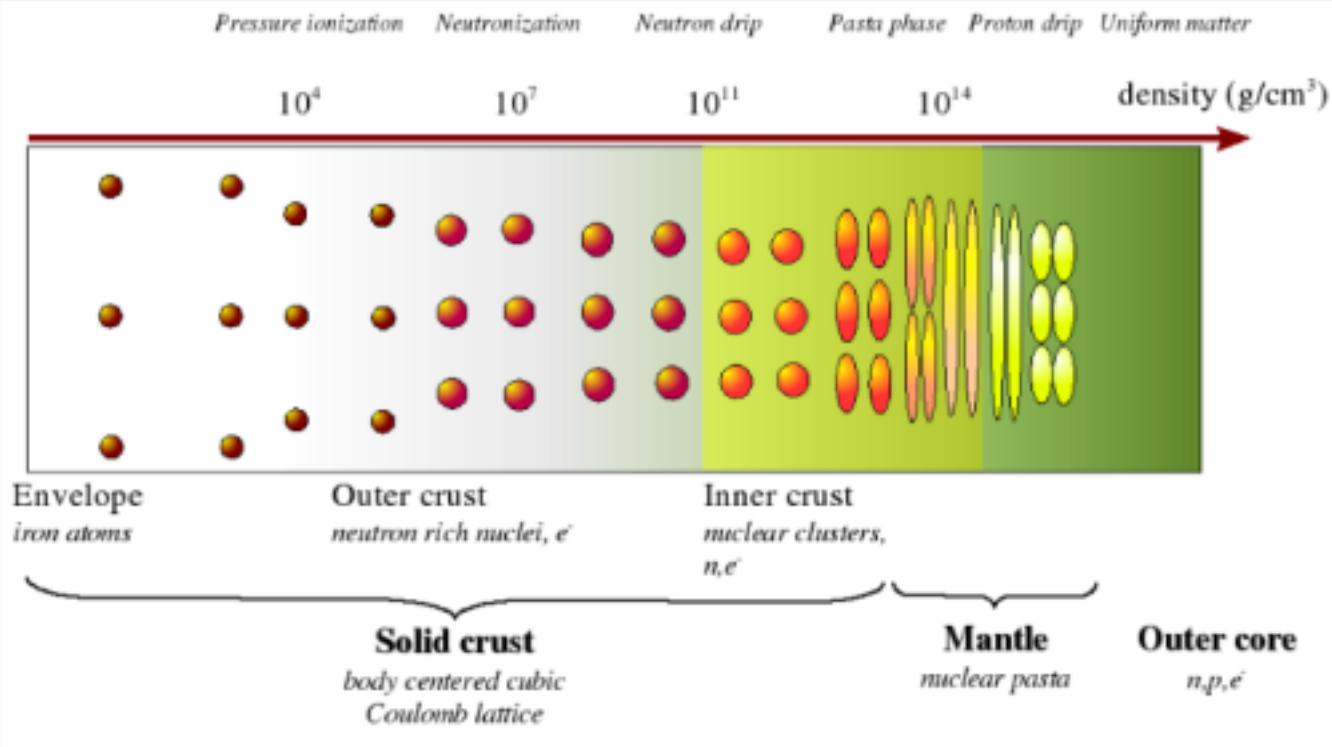

Picture from N. Chamel

- Neutron-rich nuclei
- Sea of superfluid neutrons
- Coulomb lattice
- Strong interactions
- Pasta

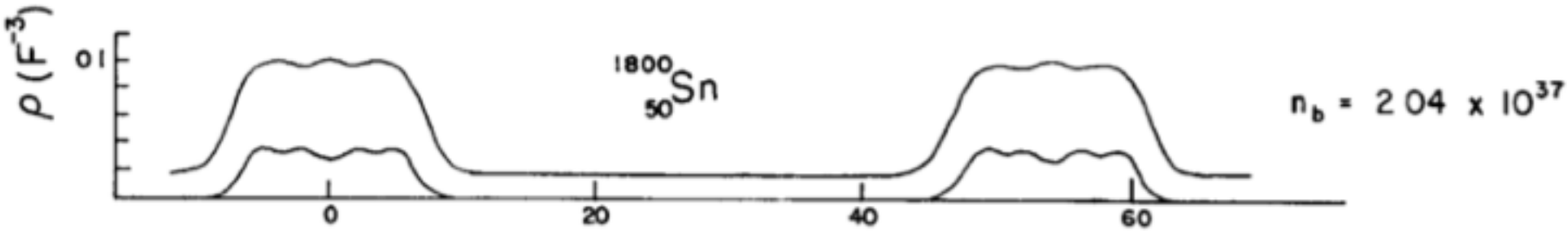

Negele and Vautherin (1973!)

Pretty much the most complicated system you can think of

Planetary masses and radii

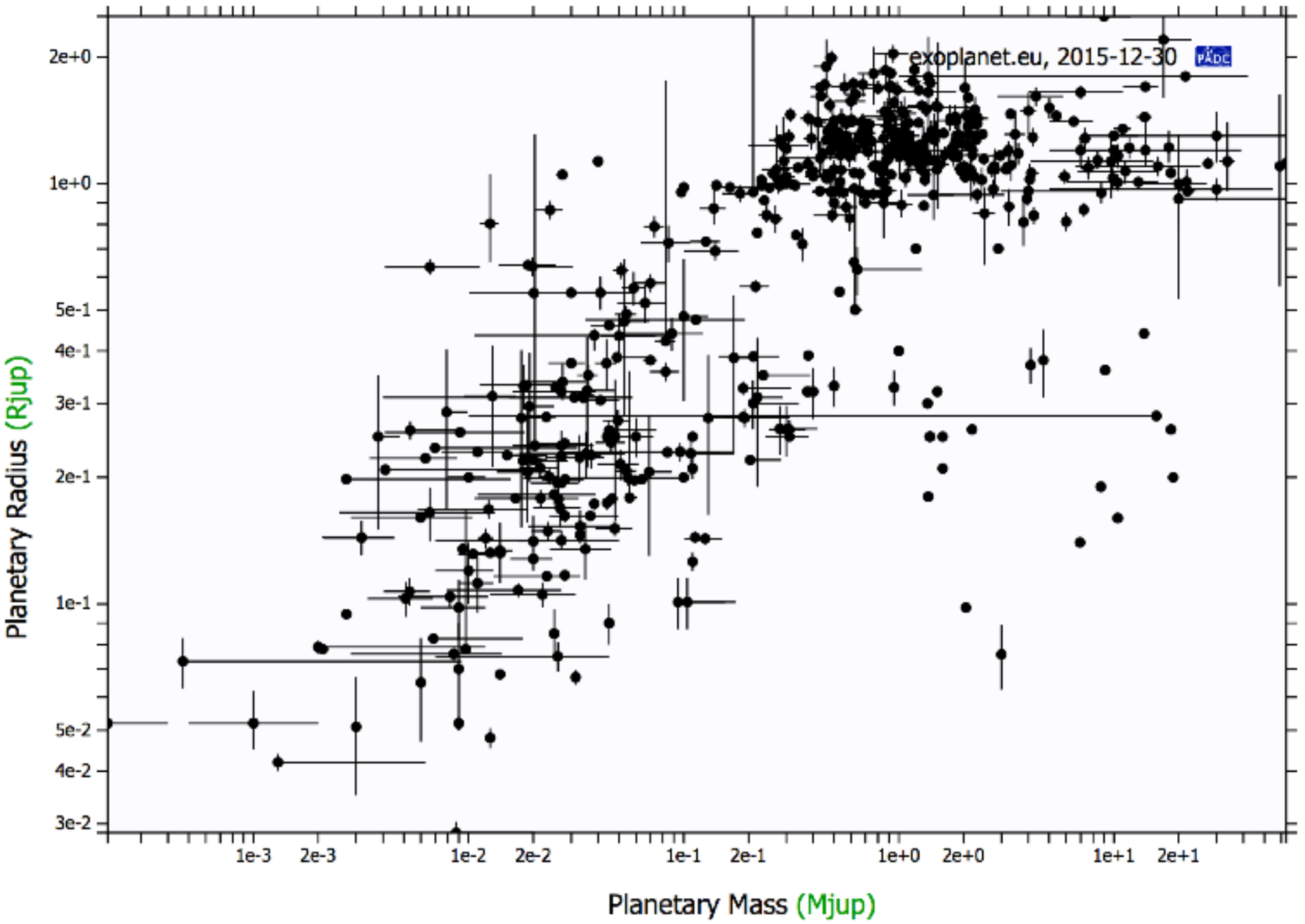

Nuclear Symmetry Energy

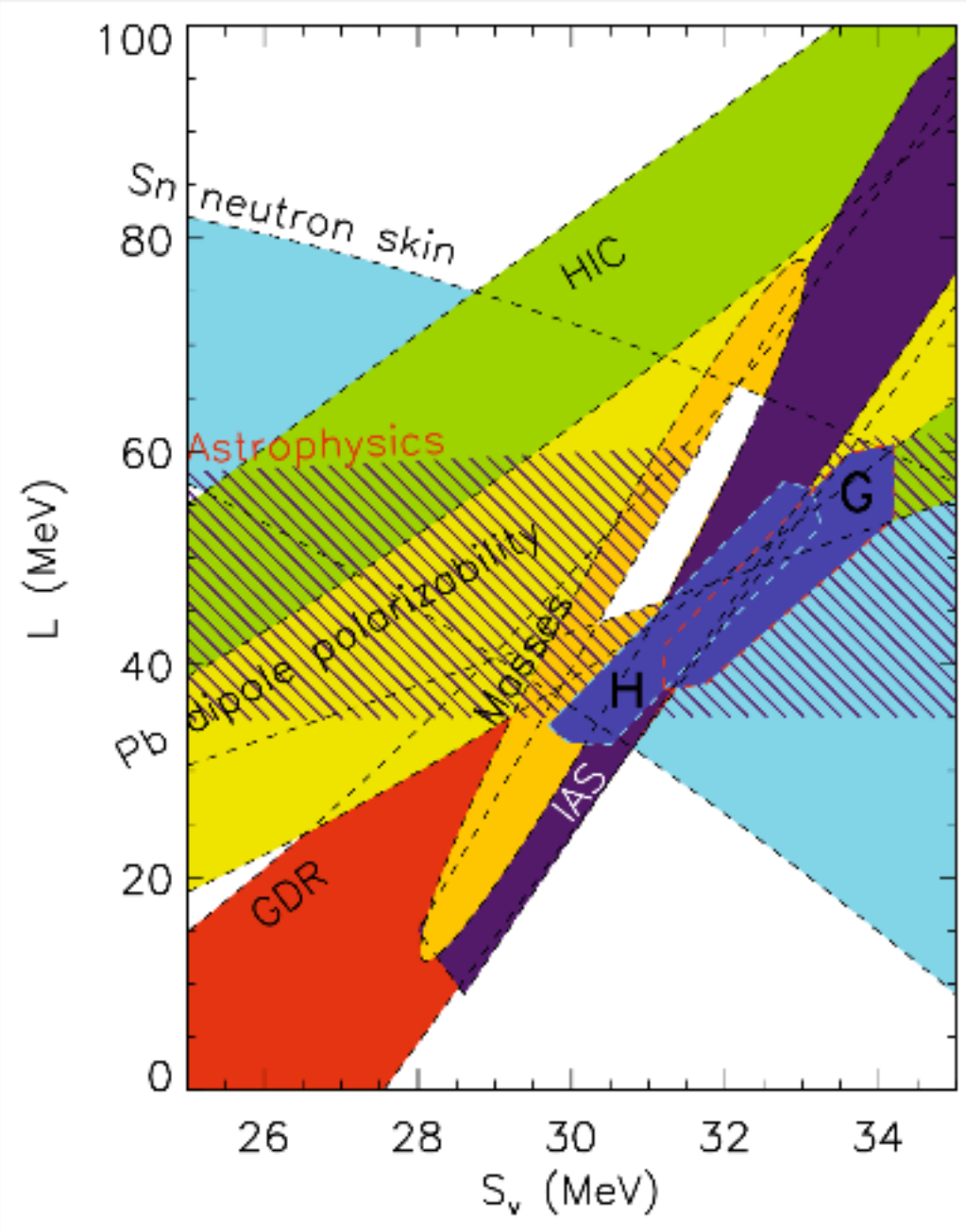

From Lattimer and Steiner (2014)

- Most uncertain part of n-n interaction near saturation
- Combined progress in experiment, theory, and observation
- All of these constraints have uncontrolled systematics
- Need to go beyond the saturation density
- Wide astrophysical impact

[based on Shetty et al. (2007), Trippa et al. (2008), Tsang et al. (2009), Chen et al. (2010), Kortelainen et al. (2010), Tamii et al. (2011), Gandolfi et al. (2012), Hebeler et al. (2012), Steiner et al. (2012), Roca-Maza et al. (2013), Danielewicz et al. (2014)]

Bridging Nuclear and Astrophysics

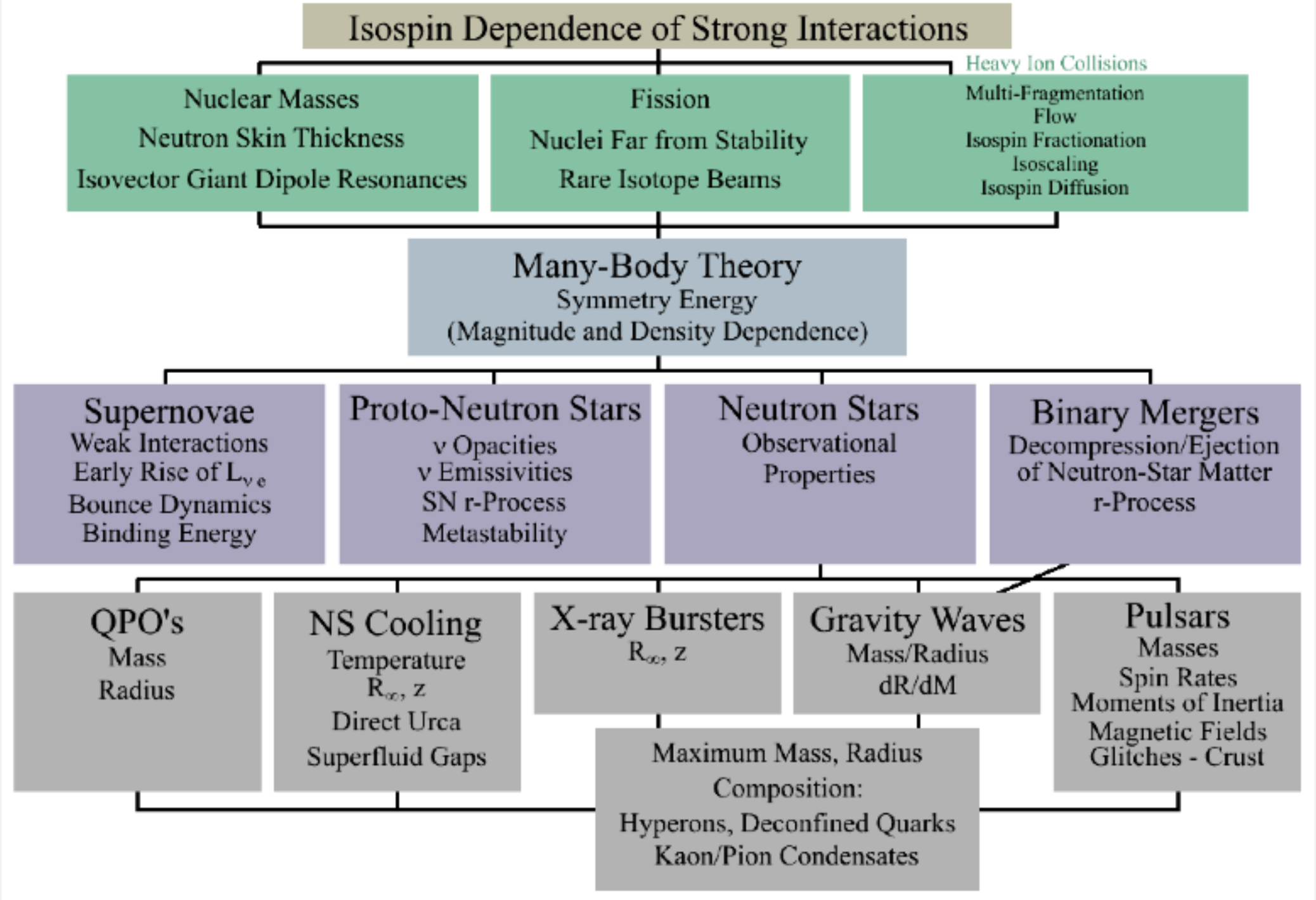

Steiner et al. (2005)

Neutron Star Tidal Deformabilities

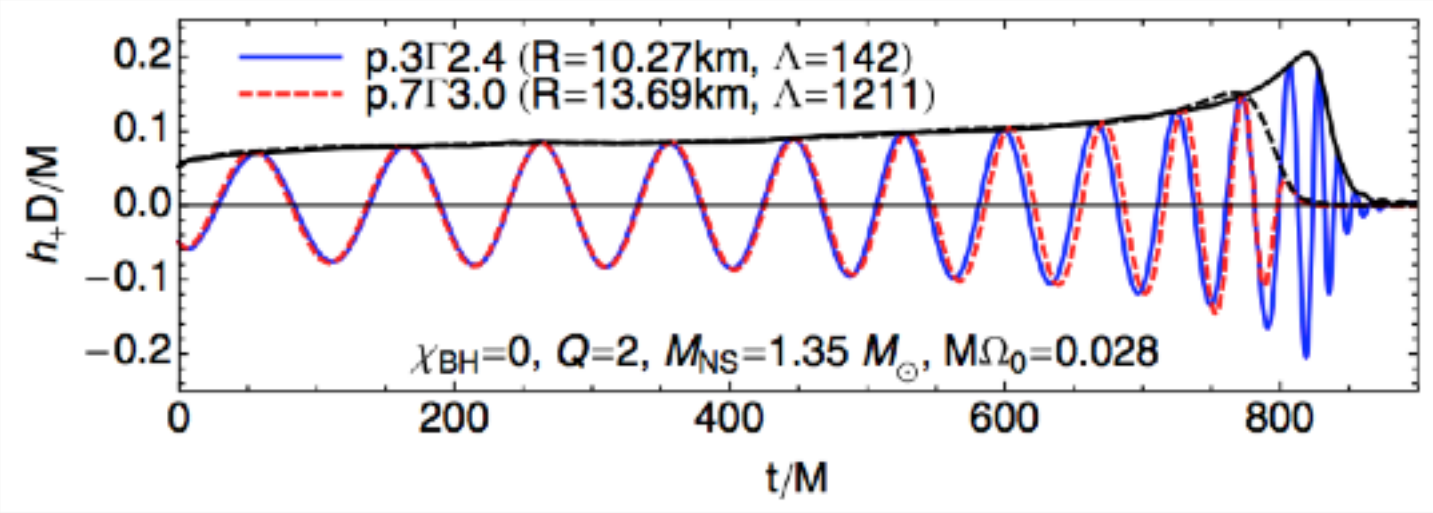

Lackey et al. (2014)

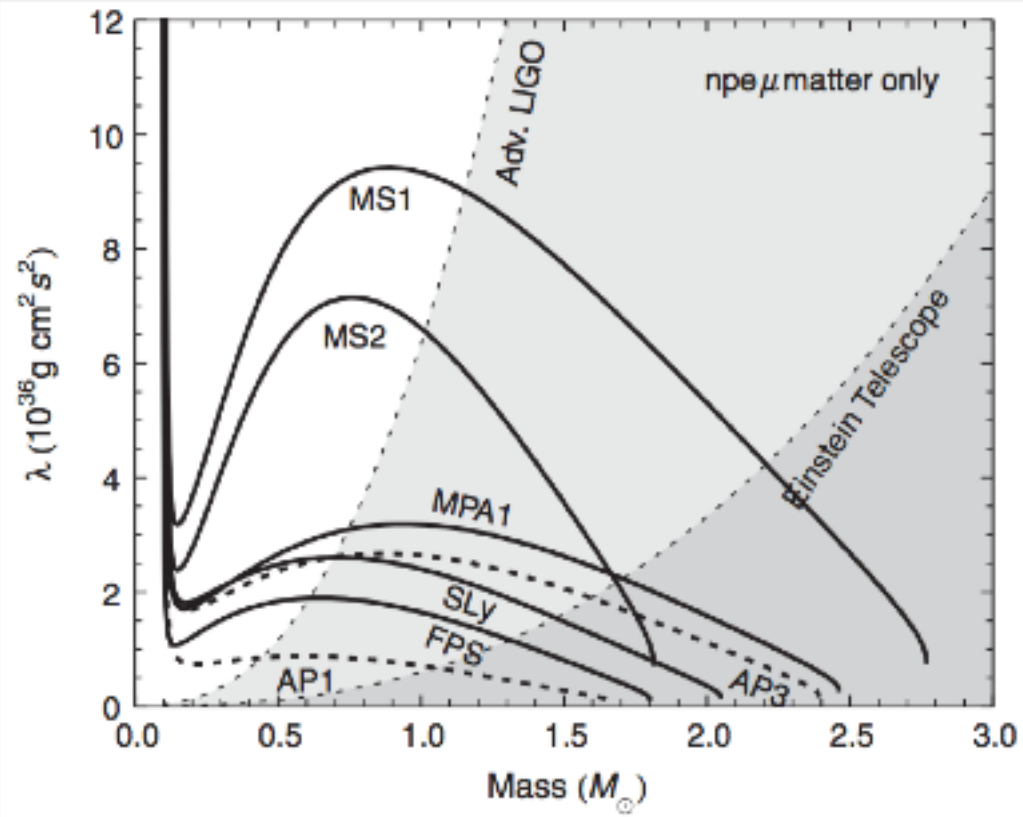

Hinderer et al. (2010)

- Gravitational wave signal from an NS merger measures tidal deformability λ
- Point masses early on; deformation near 400 Hz
- Easier to detect larger tidal deformations

New EOSs better for the r-process

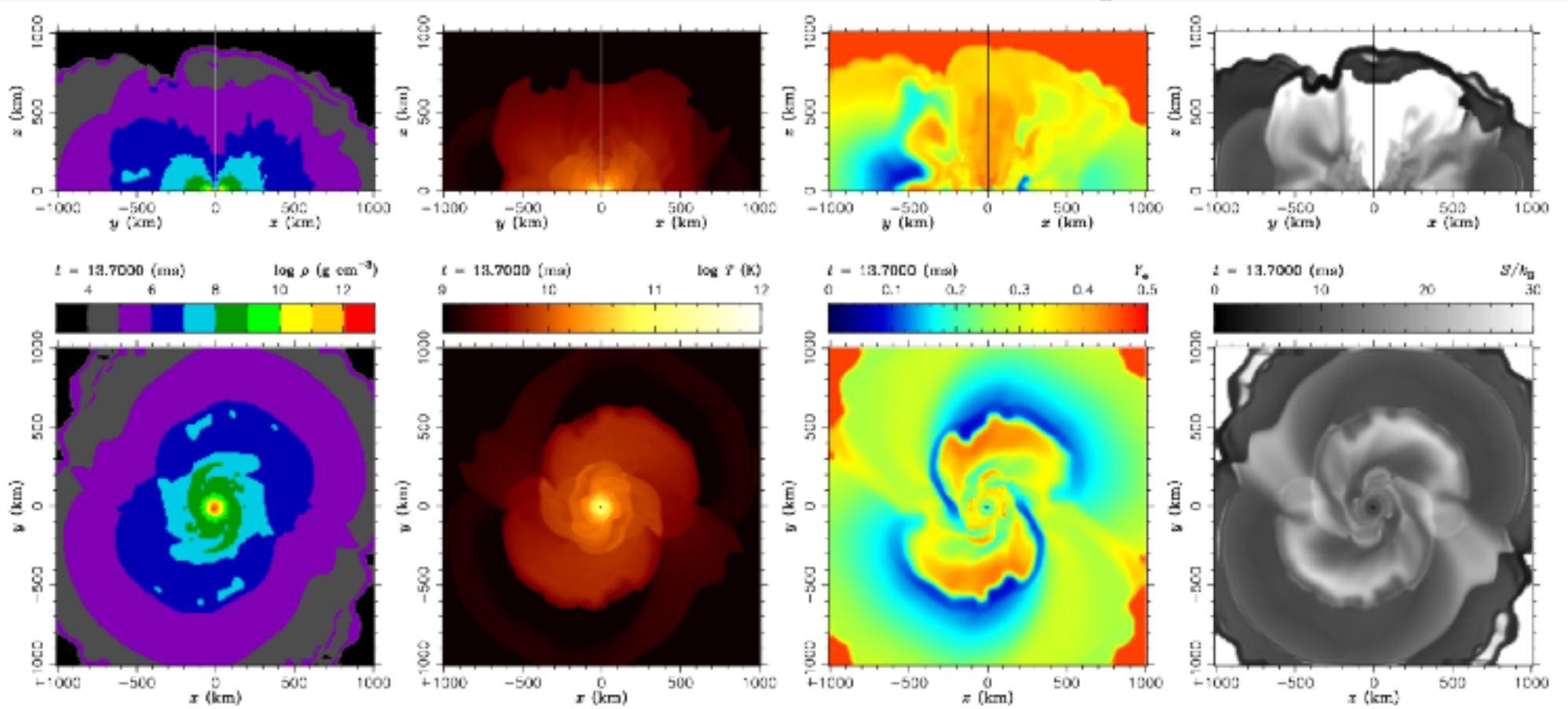

Figure 2. Color-coded distributions for density, temperature, Y_e, and S/k_B (from left to right) on the x–y (lower panels), x–z (positive sides of top panels), and y–z (negative sides of top panels) planes at the end of simulation.

- Wanajo et al. (2014) find that mergers with typical EOSs have small $Y_e \sim 0.1$, which gives an overabundance of nuclei with $A > 130$
- the SFHo EOS gives larger Y_e, and thus a r-process distribution that more closely matches observations
- L also impacts Y_e in neutrino driven winds
  Roberts et al. (2012)

Thermal Emission from Isolated Neutron Stars

- No distance measurement required
- Requires a model of the NS atmosphere to associate the observed spectrum with a luminosity or temperature

$$C_V \frac{dT}{dt} = L_\nu + L_\gamma\,, \quad L_\gamma \sim T^{2+4\alpha}\,, \quad L_\nu \sim T^8 \text{ (Modified Urca)}\,, \quad C_V \sim CT$$

- Age assumed from spin-down age or associated with a supernova remnant

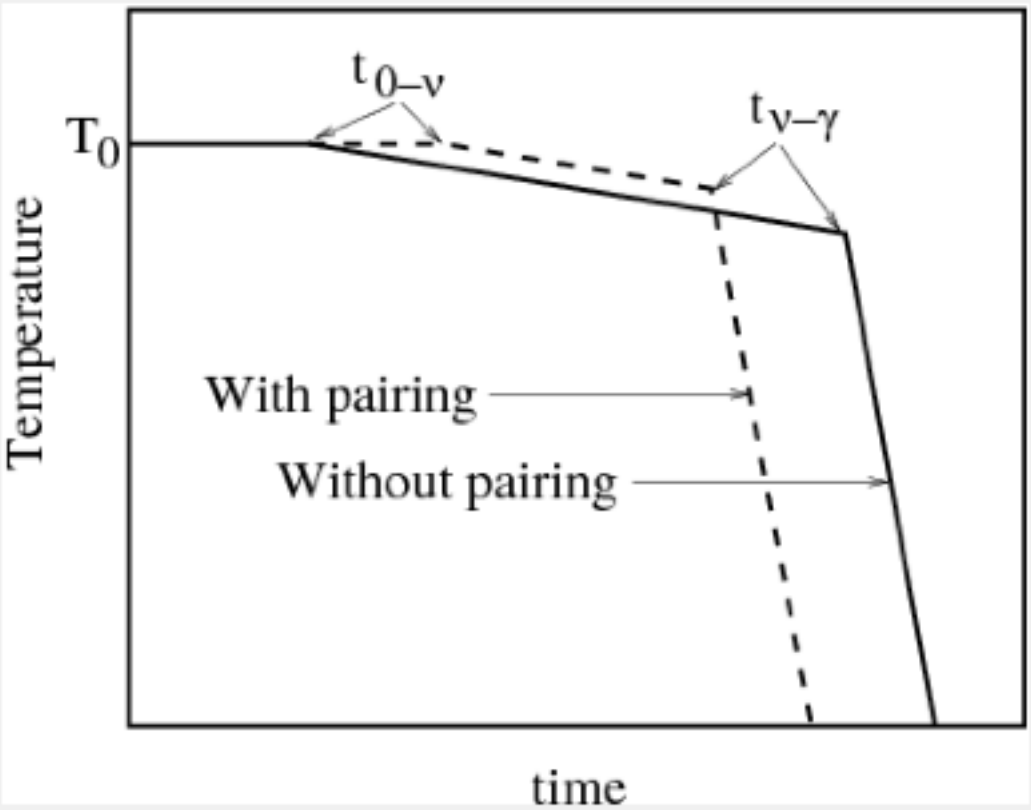

Page et al (2004)

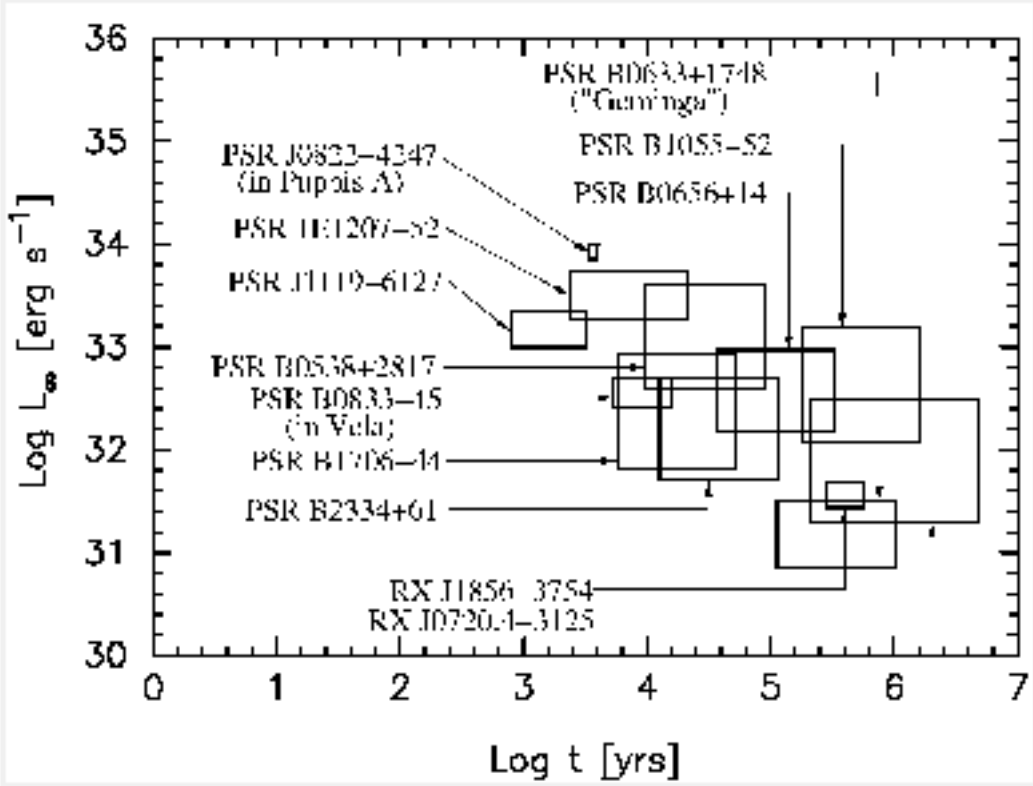

Page et al (2009)

Fitting two-dimensional data

- One-dimensional fit:

$$\chi^2 = \sum_i \left(\frac{M_i - D_i}{U_i} \right)^2; \quad \mathcal{L} \propto \exp(-\chi^2/2)$$

- Fit a data set $(t_i \pm \delta t_i, T_i \pm \delta T_i)$ to a function $T(t)$
- No unique method, typical frequentist approaches are:
  - orthogonal least-squares
  - geometric mean regression
  - Deming regression
- Bayesian generalization of several frequentist methods

$$\mathcal{L} \propto \prod_i \int dt \sqrt{\left[\left(\frac{dT}{dt} \right)^2 + 1 \right]} \exp\left\{ \frac{-[t - t_i]^2}{2\delta t_i^2} \right\} \exp\left\{ \frac{-[T(t) - T_i]^2}{2\delta T_i^2} \right\}$$

- Prior distribution manifest in the line element
- Limiting forms imply traditional χ^2 fit

Neutron Star Superfluidity

(See our review at 1302.6626)

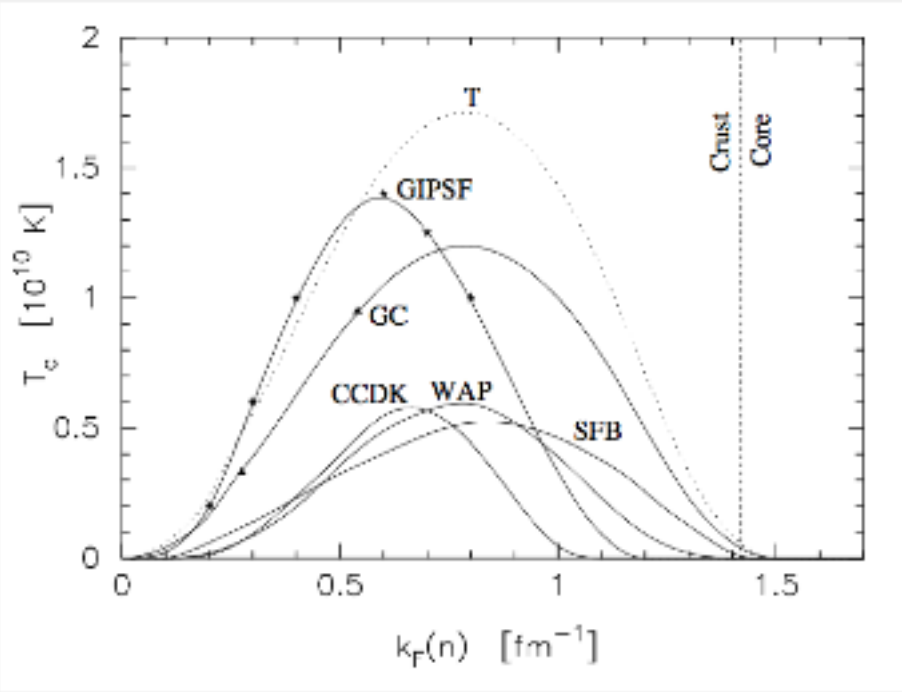

- Gap is energy gained from making a Cooper pair
- New ways of cooling

e.g. Steiner and Reddy (2009)

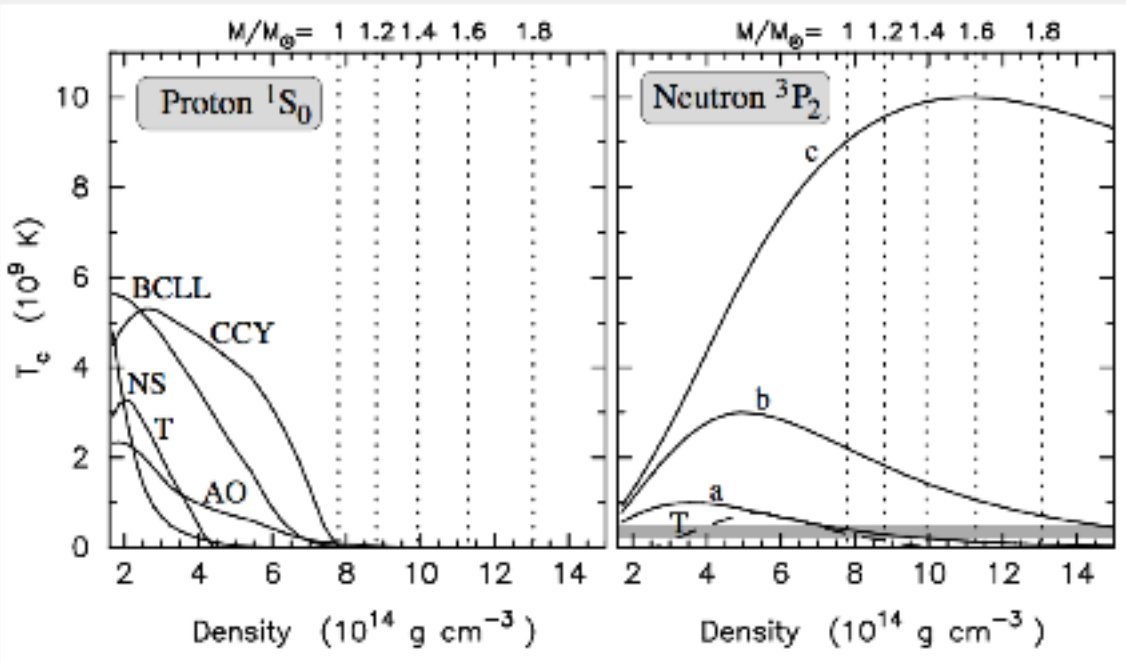

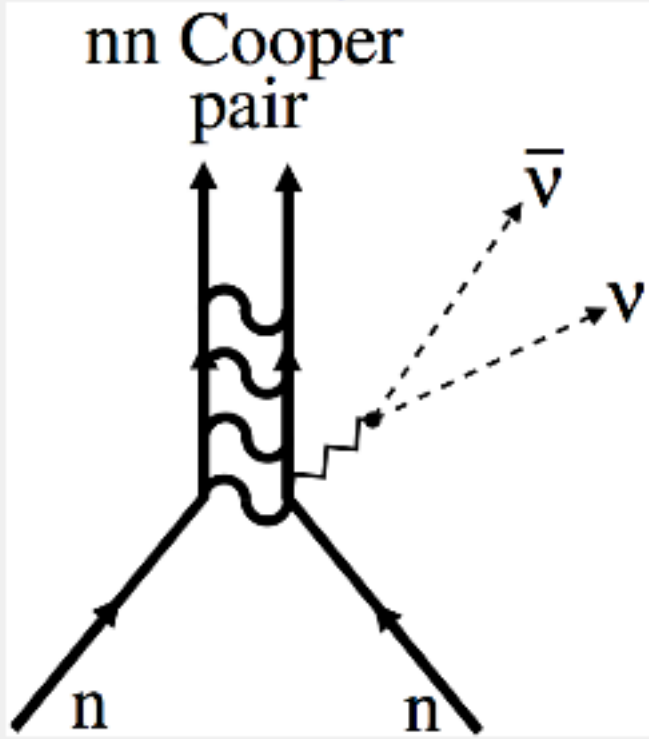

Detecting Neutron Star Superfluidity

- Data is reproduced only by a particular set of superfluid gaps, $T_{C,n} \approx 10^8$ K $T_{C,p} \approx 10^9$ K

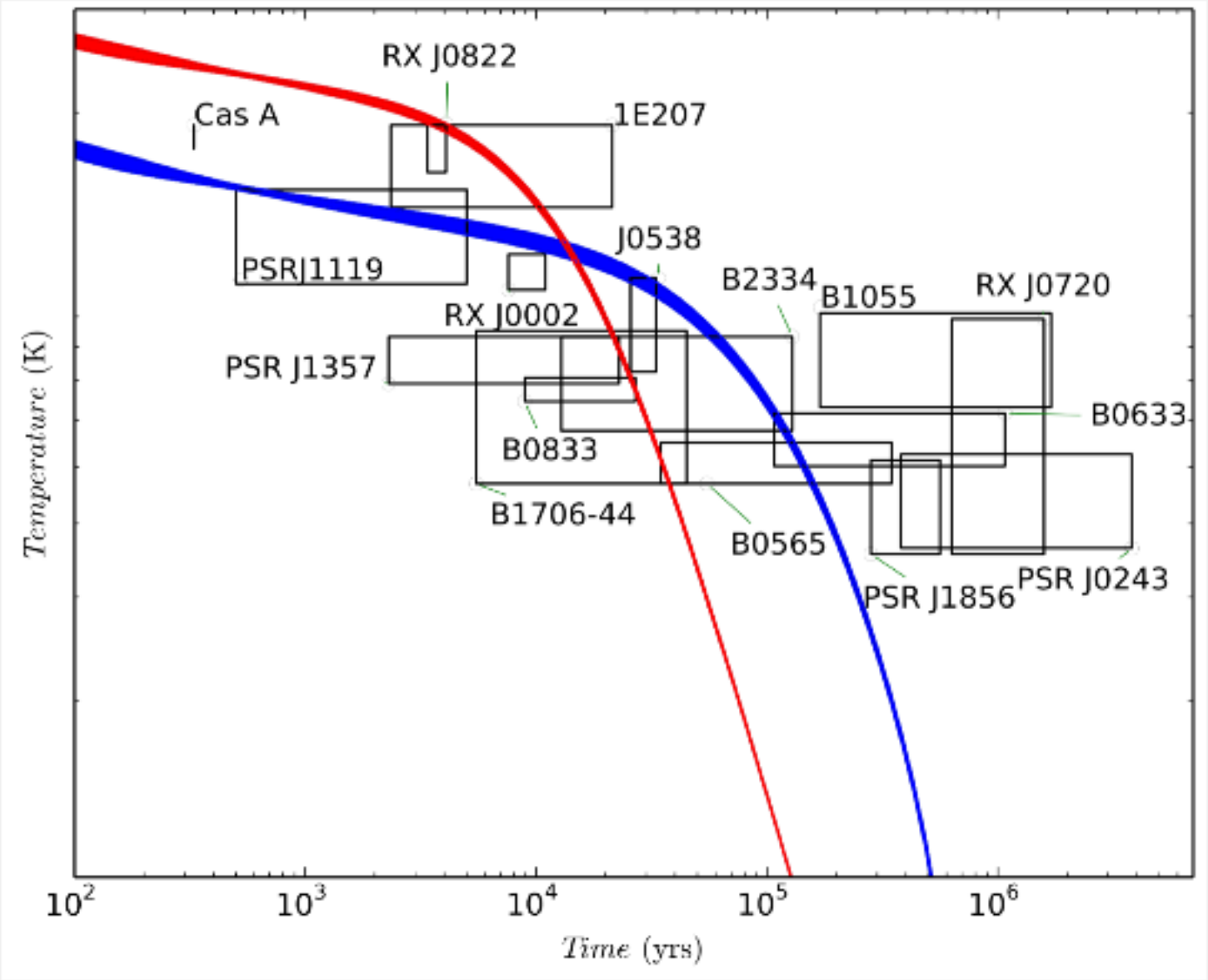

Beloin et al.

The Nuclear Symmetry Energy, Revisited

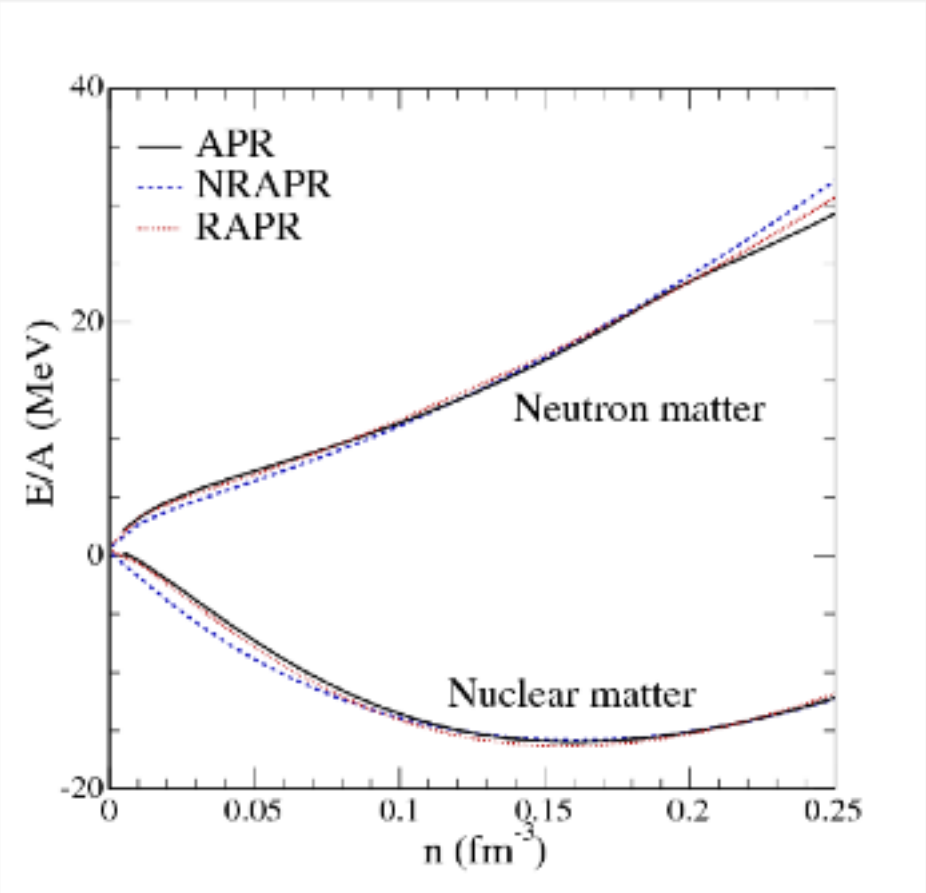

Steiner et al. (2005)

- Define $\alpha \equiv (n_n - n_p)/n$

$$S(n) = \frac{1}{2n}\left(\frac{\partial(nE/A)}{\partial\alpha}\right)_{\alpha=0}$$

- $\tilde{S}(n) = (E/A)_{\rm neut}(n) - (E/A)_{\rm nuc}(n)$
- If E/A is quadratic in α, $S(n) = \tilde{S}(n)$
- $S \equiv S(n_0)$
- L is the derivative, $L \equiv 3n_0 S'(n_0)$

- $4S(n) = \partial_\alpha \left[\mu_n(n,\alpha) - \mu_p(n,\alpha)\right]$
- $\tilde{S}(n)$ probed in neutron matter,
  $S(n)$ probed in nuclei, e.g. isovector giant dipole

Quartic Terms and the Direct Urca Process

$$(E/A)(n,\alpha) = (E/A)_{\rm nuc}(n,\alpha) + \alpha^2 S(n) + \alpha^4 Q(n)$$

- Below saturation, quartic terms are likely "small", above saturation densities, they may be important

$$\eta(n) \equiv \frac{4S(n) + 5Q(n)}{4S(n) + Q(n)}$$

- $3/7 < \eta(n) < 5$
- Complicates connection between symmetry energy and direct Urca
- Superfluidity also very important, and depends on L

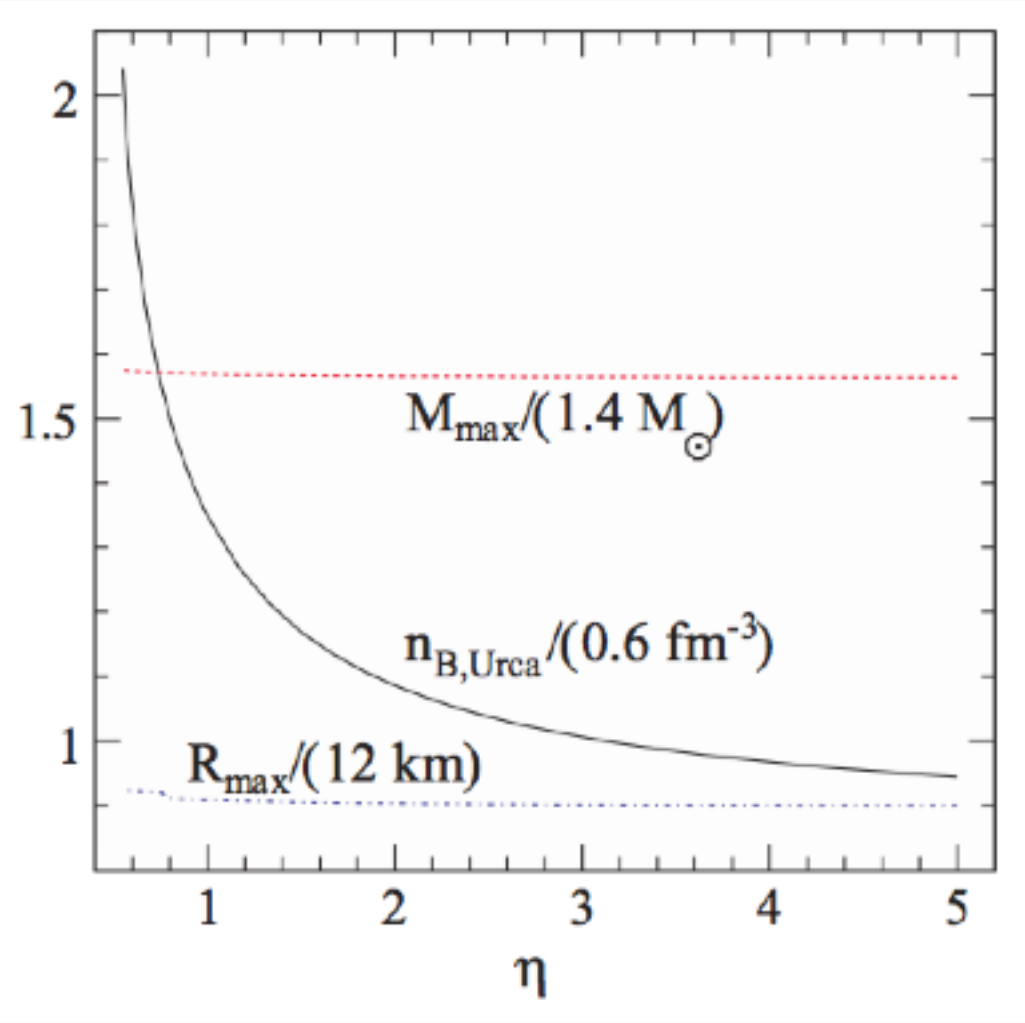

Steiner (2006)

Implications for L and radii

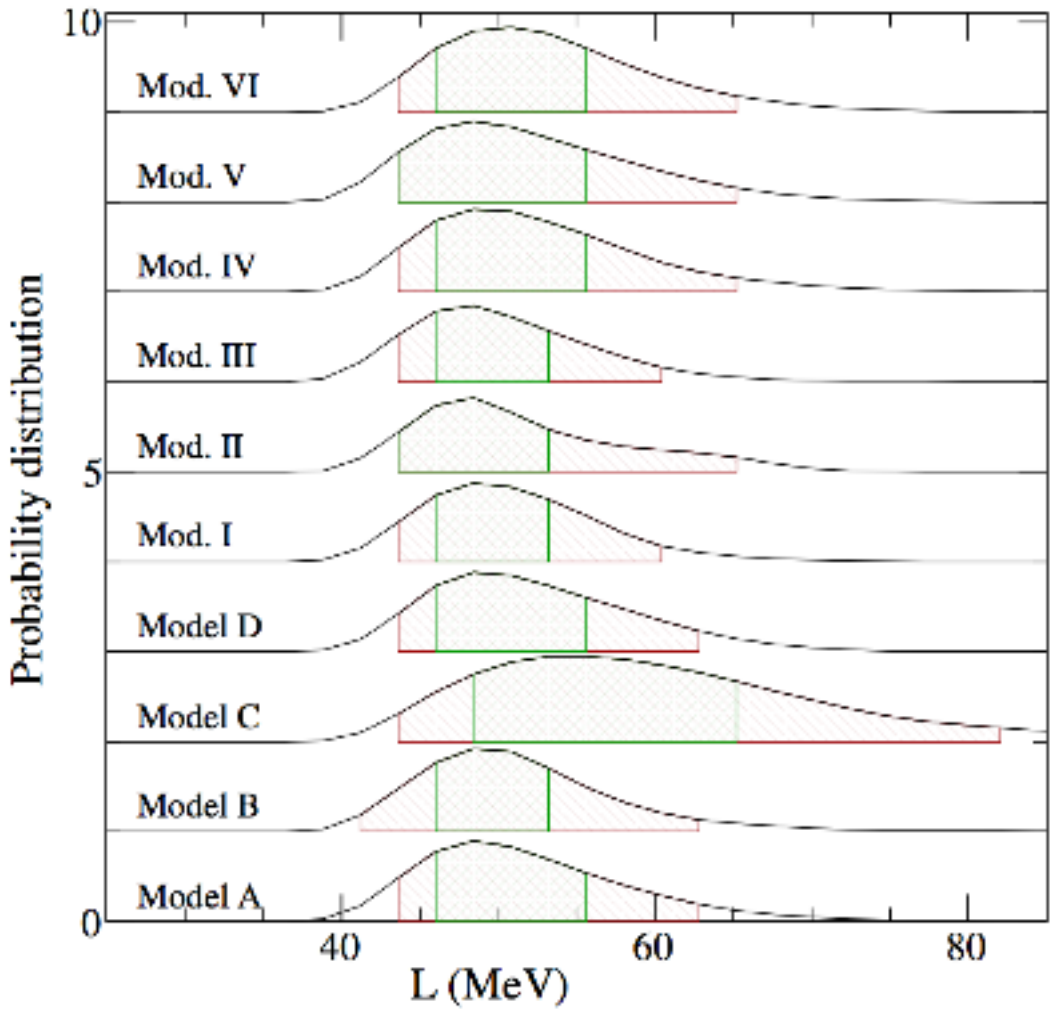

Figure 4. Limits on the density derivative of the symmetry energy, *L*. The single-hatched (red) regions show the 95% confidence limits and the double-hatched (green) regions show the 68% confidence limits.

Steiner et al. (2013)

- Trying several different prior distributions
- Model C prefers strong phase transitions
- Less certain constraints on the skin thickness of lead
- Radius of a 1.4 $M_\odot$ neutron star is about 10.5 - 13 km

Representative Models

- It has been common to use a small set of models to represent a large parameter space

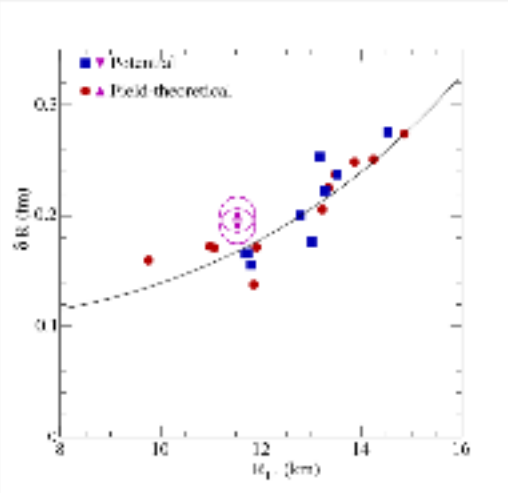

Steiner et al. (2005)

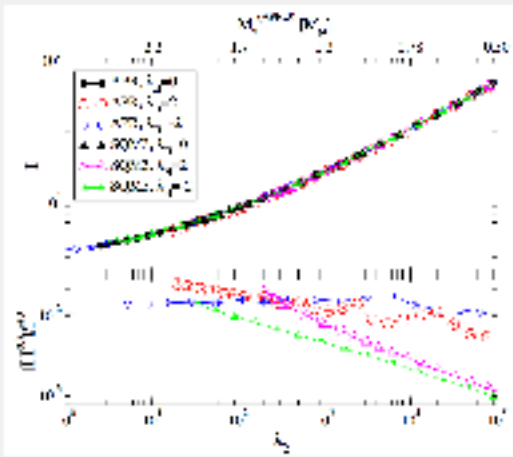

Yagi and Yunes (2015)

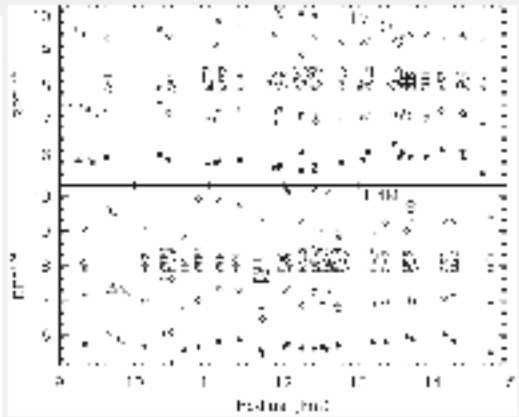

Lattimer and Prakash (2001)

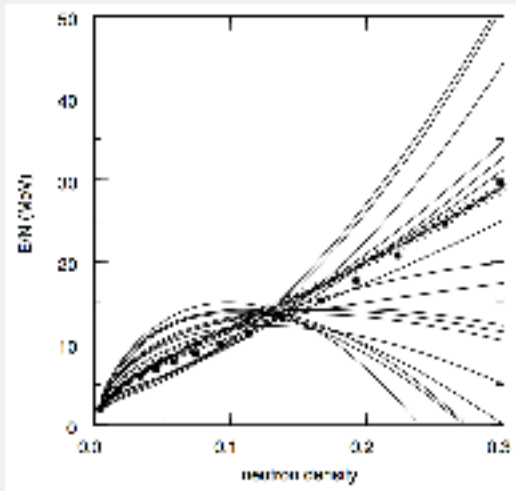

Brown (2000)

- This is like doing a many-dimensional Monte Carlo integral with only a handful of haphazard points

- New computational power has allowed for more complete explorations of parameter space